# CHAPTER - 3

# CHARACTERIZATION

## 3. INTRODUCTION

The characterization of a catalyst is an important part of catalytic research and development programme Now-a-days novel techniques and sophisticated instruments are used to characterize the catalyst structure before, during and after the use These developments have resulted in a better understanding of the catalytic phenomenon. The application of advanced electronic and computer analysis has optimized many of these analytical tools. Thus, the difficult goal of revealing the relationship between the structure and reactivity of the catalytic material is finally within the reach. However, complete characterization of supported catalysts is extremely difficult due to inhomogeneous nature of the catalysts themselves Accordingly, a wide range of analytical and spectroscopic techniques have been applied to the problem [1,2]

The characterization of a catalyst provides information on three distinct but related sorts These are chemical composition and structure, texture and mechanical properties and catalytic activity

Chemical composition and structure refer to the elemental composition, properties of individual phases present, surface composition, nature and properties of surface functional groups. The structure of the catalyst refers to its geometric structure and morphology. The characterization of a catalyst in terms

of its activity is the quantification of its ability to carry out a particular chemical transformation under a specified condition

The present chapter deals with the physico-chemical characterization of polymer bound complexes such as chemical composition, moisture content, apparent bulk density, surface area and swelling studies Spectroscopic studies have been utilized to investigate the coordination structure of the polymer supported metal complexes and oxidation state of the metal atom using techniques such as, UV-Vis, FTIR, and ESR Thermal stability of the support and supported catalysts has been studied by the use of DTA and TG analysis SEM has been used for the morphology of the support and supported complexes

The chemical modification of crosslinked chloromethylated poly(styrene-divinylbenzene) and the loading of metal onto this support was carried out as per the sequence shown in **Chapter 2, Scheme 2.1.** Twelve novel catalysts were prepared and studied They have been designated as given in **Chapter 2 .**

## 3.1 CATALYST CHARACTERIZATION

### 3.1.1 SURFACE AREA MEASUREMENT

Most catalysts of practical importance are highly porous and posses large specific surface areas Although the catalytic activity may be only indirectly related to this "total" surface, the determination of surface area is generally considered to be an important requirement in catalyst characterization [3] Adsorption method was used for the measurement of total surface area and pore size of polymer support and polymer bound catalysts Adsorption-desorption isotherms of nitrogen were recorded on a Carlo-Erba Surface Analyzer Series-1900 at liquid nitrogen temperature (i e -196$^0$C), after degassing the sample at 80 $^o$C for 4 h From the isotherms, specific surface area and pore volume were calculated using BET equation The results are given in **Table 3.1.** A decrease in the surface area was observed for all the catalysts when compared to that of the respective supports It may be due to blocking of pores of the support by successive introduction of Schiff base ligand and metal on the polymer matrix This is in accordance with the results obtained earlier by Ram et al [4-6] Moreover, the surface area of catalyst bearing 1,3-diaminopropane Schiff bases have been found to be lower than those derived from 4,4'-diaminobiphenyl . This difference is attributed to the relative size difference in the two types of Schiff bases formed on the polymer matrix [7,8].

**Table 3.1**
**Surface area and pore volume of supports and supported catalysts**

| Catalyst | Surface area ($m^2 g^{-1}$) | Pore volume ($cm^3 g^{-1}$) |
|---|---|---|
| 5% P(S-DVB)$CH_2Cl$ | 39 9 | 0 20 |
| 8% P(S-DVB)$CH_2Cl$ | 52 2 | 0 21 |
| Ru-A | 34 8 | 0 12 |
| Ru-B | 48 9 | 0 15 |
| Ru-C | 34 9 | 0 12 |
| Ru-D | 40 4 | 0 13 |
| Mn-A | 31 8 | 0 12 |
| Mn-B | 45 9 | 0 10 |
| Mn-C | 34 3 | 0 13 |
| Mn-D | 51.3 | 0 15 |
| Pd-A | 30 5 | 0 12 |
| Pd-B | 38 2 | 0 15 |
| Pd-C | 34 6 | 0 10 |
| Pd-D | 45 4 | 0 13 |

### 3.1.2 CHEMICAL COMPOSITION

The attachment of Schiff base derived from 1,3-diaminopropane and 4,4'-diaminobiphenyl and salicylaldehyde on the functionalised polymer was confirmed by their elemental analysis The elemental analysis at various stages are given in **Table 3.2 to 3.4.** The results show the higher percentage of nitrogen in catalyst **A** and **C** as compared to that in **B** and **D.** This is attributed to the lower degree of crosslinking in the former ( 5% in **A** and **C** as against 8% in **B** and **D** ). This can be explained as follows. In the case of polymer supports with higher degree of crosslinking, the network has a dense and relatively large number of inaccessible domains resulting into lower functionalization [9].

### 3.1.3 SWELLING STUDIES

In order to optimize the rate and specificity of a particular catalyst system, it is necessary to consider many factors. The nature of the solvent used plays an important role in the rate of reaction. Swelling is a very useful parameter to control both specificity and selectivity in a batch reactor.

To achieve higher activity and selectivity with polymer bound catalysts, it is necessary that the reactant molecules have accessibility to all catalytic sites

**Table 3.2**
**Elemental analysis of chloromethylated polymers, their Schiff bases and supported Ru(III) catalysts**

| Compound | C% | H% | Cl% | N% | Ru(g/g resin) |
|---|---|---|---|---|---|
| 5% P(S-DVB)$CH_2Cl$ | 74 2 | 6 0 | 15 6 | - | - |
| 8% P(S-DVB)$CH_2Cl$ | 72 8 | 6 0 | 27 6 | - | - |
| 5% P(S-DVB)(1,3-dap-SB) | 81 6 | 7 3 | 10 9 | 4 9 | - |
| 8% P(S-DVB)(1,3-dap-SB) | 78 1 | 6 2 | 13.4 | 4 7 | - |
| 5% P(S-DVB)(4,4'-dabp-SB) | 80.1 | 7 0 | 09 7 | 4.9 | - |
| 8% P(S-DVB)(4,4'-dabp-SB) | 75 6 | 6 1 | 13 9 | 2 4 | - |
| **Ru-A** | 72 8 | 7 3 | - | 3 9 | $7\ 7x10^{-4}$ |
| **Ru-B** | 70 9 | 6 2 | - | 3 0 | $3.5x10^{-4}$ |
| **Ru-C** | 72 9 | 7 1 | - | 2 1 | $6\ 0x10^{-4}$ |
| **Ru-D** | 70 0 | 5 9 | - | 1 9 | $4\ 1x10^{-4}$ |

**Table 3.3**
**Elemental analysis of chloromethylated polymer, their Schiff bases and supported Mn(II) catalysts**

| Compound | C% | H% | Cl% | N% | Mn(g/g resin) |
|---|---|---|---|---|---|
| 5% P(S-DVB)$CH_2Cl$ | 74 2 | 6.0 | 15.6 | - | - |
| 8% P(S-DVB)$CH_2Cl$ | 72 8 | 6 0 | 27 6 | - | - |
| 5% P(S-DVB)(1,3-dap-SB) | 81 6 | 7 3 | 10 9 | 4 9 | - |
| 8% P(S-DVB)(1,3-dap-SB) | 78 1 | 6 2 | 13 4 | 4 7 | - |
| 5% P(S-DVB)(4,4'-dabp-SB) | 80 1 | 7.0 | 09 7 | 4 9 | - |
| 8% P(S-DVB)(4,4'-dabp-SB) | 75 6 | 6 1 | 13 9 | 2 4 | - |
| **Mn-A** | 73 5 | 6 9 | - | 4 2 | $7\ 0x10^{-4}$ |
| **Mn-B** | 71 9 | 6 0 | - | 4 0 | $3\ 2x10^{-4}$ |
| **Mn-C** | 73 6 | 7 0 | - | 2.0 | $7\ 5x10^{-4}$ |
| **Mn-D** | 69 9 | 5 9 | - | 1 9 | $5\ 1x10^{-4}$ |

**Table 3.4**
**Elemental analysis of chloromethylated polymer, their Schiff bases and supported Pd(II) catalysts**

| Compound | C% | H% | Cl% | N% | Pd(g/g resin) |
|---|---|---|---|---|---|
| 5% P(S-DVB)$CH_2Cl$ | 74 2 | 6 0 | 15 6 | - | - |
| 8% P(S-DVB)$CH_2Cl$ | 72 8 | 6 0 | 27 6 | - | - |
| 5% P(S-DVB)(1,3-dap-SB) | 81.6 | 7 3 | 10 9 | 4 9 | - |
| 8% P(S-DVB)(1,3-dap-SB) | 78.1 | 6.2 | 13 4 | 4 7 | - |
| 5% P(S-DVB)(4,4'-dabp-SB) | 80 1 | 7 0 | 09.7 | 4 9 | - |
| 8% P(S-DVB)(4,4'-dabp-SB) | 75 6 | 6 1 | 13 9 | 2 4 | - |
| **Pd-A** | 71.9 | 7 1 | - | 4 0 | $1\ 0 \times 10^{-4}$ |
| **Pd-B** | 72 1 | 6 0 | - | 3 2 | $2\ 5 \times 10^{-4}$ |
| **Pd-C** | 72 0 | 6 9 | - | 3 0 | $2\ 0 \times 10^{-4}$ |
| **Pd-D** | 70 8 | 6 3 | - | 2.3 | $1.7 \times 10^{-4}$ |

both on the surface and the interior of the beads. This requires the use of a suitable solvent in which the polymer has maximum swelling so that the matrix expands sufficiently to allow to the reactant molecules to diffuse within the solvent channel and encounter the catalytic site

The extent of swelling depends on the polymer-solvent interaction which is determined not only by the nature of solvent and polymer matrix but also by the active groups attached to the polymer matrix

Exhaustive swelling studies were carried out for supports and the supported catalysts using solvents of different polarity Polar solvents were generally found to be very good swelling agents for all the catalysts than the non-polar solvents like heptane, benzene, etc The results are given in **Table 3.5 to 3.7.** This is on the expected lines because with increase in the degree of crosslinking of the polymer support, the percentage swelling decreases, indicating the rigid nature of the support Thus, the solvent of choice should combine good swelling ability and high polarity for catalytic use Accordingly dichloromethane, acetonitrile and methanol were chosen as solvents for carrying out catalytic reactions and also to overcome miscibility problem with the reactant

**Table 3.5**
**Swelling data of supported catalysts (mol%)**

| Solvent | Catalysts | | | |
|---|---|---|---|---|
| | Ru-A | Ru-B | Ru-C | Ru-D |
| Water | 6 57 | 6 01 | 6 43 | 6 64 |
| Methanol | 4 99 | 4 31 | 4.77 | 4 51 |
| Ethanol | 4.19 | 4 31 | 4.36 | 3 30 |
| Acetonitrile | 3 68 | 3 38 | 3 06 | 2 78 |
| Dichloromethane | 2.96 | 2 88 | 3 01 | 2 91 |
| Dioxane | 2 94 | 4 18 | 3.30 | 2 86 |
| DMF | 3 15 | 2 74 | 3 16 | 2 13 |
| Acetone | 2.84 | 2 61 | 2 68 | 2.48 |
| THF | 1.85 | 1 84 | 1 77 | 1 74 |
| Benzene | 1 41 | 1 50 | 1 32 | 0 97 |
| Cyclohexane | 1 89 | 1.78 | 1 38 | 1 41 |
| n-heptane | 0 91 | 0 93 | 0 74 | 0 75 |

**Table 3.6**
**Swelling data of supported catalysts (mol%)**

| Solvent | Catalysts | | | |
|---|---|---|---|---|
| | Mn-A | Mn-B | Mn-C | MN-D |
| Water | 6 22 | 6 7 I | 8 01 | 6 68 |
| Methanol | 5 30 | 4 62 | 5 92 | 5 17 |
| Ethanol | 3 07 | 3 41 | 3 38 | 3 60 |
| Acetonitrile | 2 90 | 2 79 | 2.72 | 3 79 |
| Dichloromethane | 2 88 | 2 80 | 2 76 | 3 50 |
| Dioxane | 2.31 | 3.17 | 2 86 | 3 11 |
| DMF | 3.60 | 2 93 | 2 97 | 3.66 |
| Acetone | 2 52 | 2.79 | 2 76 | 2.77 |
| THF | 2 78 | 1.82 | 2 33 | 1 82 |
| Benzene | 1 77 | 1 37 | 1 88 | 1 36 |
| Cyclohexane | 2 18 | 1 66 | 1 12 | 1 58 |
| n-heptane | 0.99 | 0 81 | 1 10 | 0 74 |

**Table 3.7**
**Swelling data of supported catalysts (mol%)**

| Solvent | Catalysts | | | |
|---|---|---|---|---|
| | Pd-A | Pd-B | Pd-C | Pd-D |
| Water | 6.67 | 6.15 | 6 79 | 6 26 |
| Methanol | 5 06 | 4 45 | 5 39 | 4 32 |
| Ethanol | 4 06 | 3 72 | 3 41 | 5 02 |
| Acetonitrile | 3 73 | 3 36 | 3 12 | 3.43 |
| Dichloromethane | 3 80 | 3 40 | 3 01 | 3 10 |
| Dioxane | 2 99 | 3 15 | 2 66 | 3 02 |
| DMF | 3 12 | 2 60 | 2 46 | 2 74 |
| Acetone | 2 84 | 3 15 | 2 36 | 2 68 |
| THF | 1 94 | 2 16 | 1 90 | 1.63 |
| Benzene | 1 59 | 1 79 | 1 65 | 1 41 |
| Cyclohexane | 2 68 | 1 80 | 1 59 | 1 41 |
| n-heptane | 0 82 | 1 31 | 1 51 | 0 84 |

### 3.1.4 APPARENT BULK DENSITY AND MOISTURE CONTENT

One of the primary objectives of the engineers who design the industrial reactors is to precisely determine the catalytic-bed dimensions The catalyst bed is characterized not only by its diameter and height but also by its density When the polymer supported catalyst is employed in a liquid slurry reactor, the apparent bulk density may not play significant role because of the higher volume occupied by swollen polymer than the dry polymer as also the swelling capacity differs from solvent to solvent Apparent bulk density and percentage moisture of all polymer supports and catalysts are given in **Table 3.8.**

### 3.1.5 SPECTRAL CHARACTERIZATION

#### 3.5.1.1 UV-VISIBLE SPECTROSCOPY

The interaction of light with catalyst particles is regarded as a major tool in the characterization of catalyst. The transition involved in the UV-visible region are electronic. Thus, d-d transitions observed when degenerate d-orbitals split by placing a transition metal ion in crystal field. The splitting of the energy levels is affected by the number of d electrons, the effective charge on the ion, the distribution and the charge of the surrounding ions These transitions usually

**Table 3.8**
**Apparent bulk density and moisture content of polymer supported catalysts**

| Catalyst | Moisture content(wt%) | Apparent bulk density (g $cm^{-3}$) |
|---|---|---|
| Ru-A | 0 33 | 0 43 |
| Ru-B | 0.37 | 0 49 |
| Ru-C | 0 36 | 0 45 |
| Ru-D | 0 34 | 0 49 |
| Mn-A | 0 39 | 0 44 |
| Mn-B | 0 37 | 0 50 |
| Mn-C | 0 24 | 0 43 |
| Mn-D | 0 37 | 0.49 |
| Pd-A | 0 31 | 0 45 |
| Pd-B | 0 48 | 0 49 |
| Pd-C | 0.30 | 0 45 |
| Pd-D | 0 25 | 0 52 |

occur in the visible part of the spectrum Charge transfer transitions involve more than one atom and include transition from metal to ligand or vice versa, or between two neighbouring metal atoms of different oxidation states Usually such transitions occur in the UV region and do not mask the d-d transition in the visible region The technique employed in the UV-visible spectroscopy for powdered samples involves the measurement of diffusely reflected light [10]. In supported catalysts, UV-visible spectra are normally interpreted by comparison with the spectra of corresponding homogeneous complexes

The UV-vis reflectance spectra of the newly synthesized catalysts in $BaSO_4$ matrix exhibit weak intensity absorption bands in the region 380 nm for ruthenium supported, 330 nm for palladium supported and 395 nm for manganese supported catalysts, which are assigned to the d-d transition of the metal **(Fig. 3.1- 3.3).** Ligand to metal charge transfer bands (LMCT) were not seen in this region

### 3.1.5.2 INFRARED SPECTROSCOPY

Infrared spectroscopy is most widely used technique for the study of supported metal complex catalysts It is used to study adsorbed molecules and their binding with catalyst surface It provides reliable information about organic compounds in the mid-IR (4000-600 $cm^{-1}$) region and that of the metal-ligand vibrations in far-IR(600-50 $cm^{-1}$) region The bond formed between the metal

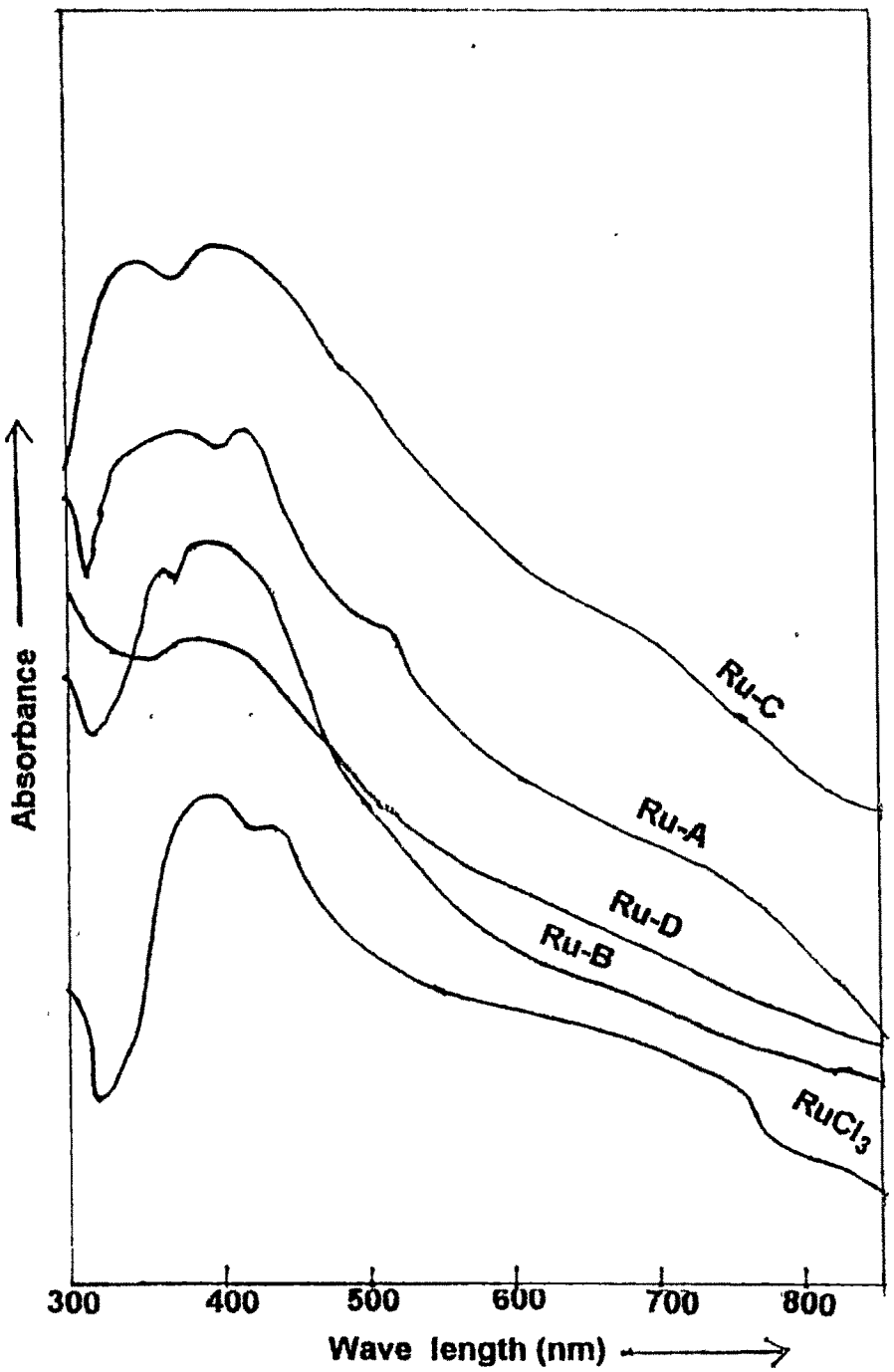


Fig 3.1 : UV-VIS spectra of Ru(III)-Schiff base complexes

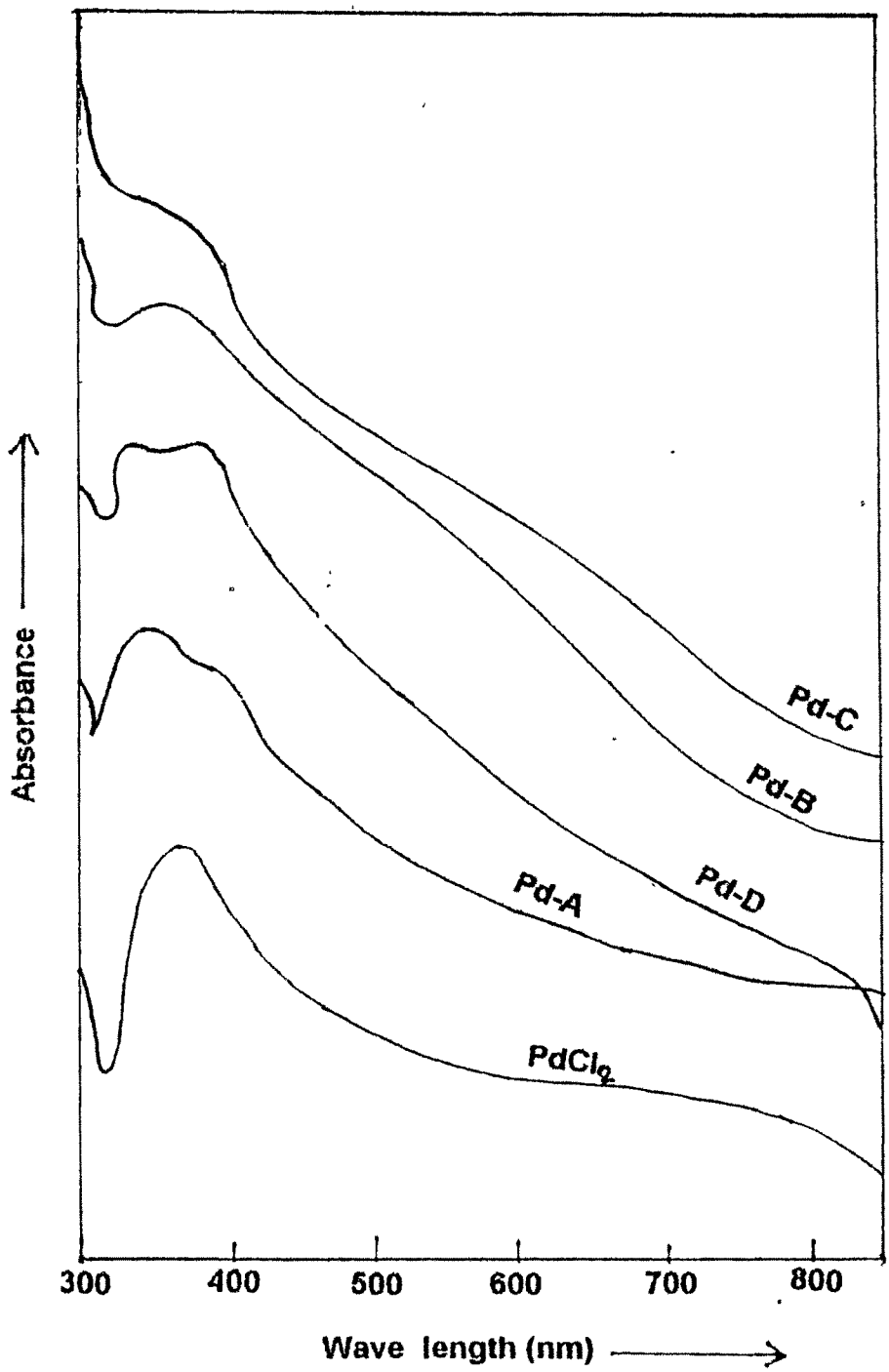


**Fig 3.2 : UV-VIS spectra of Pd(II)-Schiff base complexes**

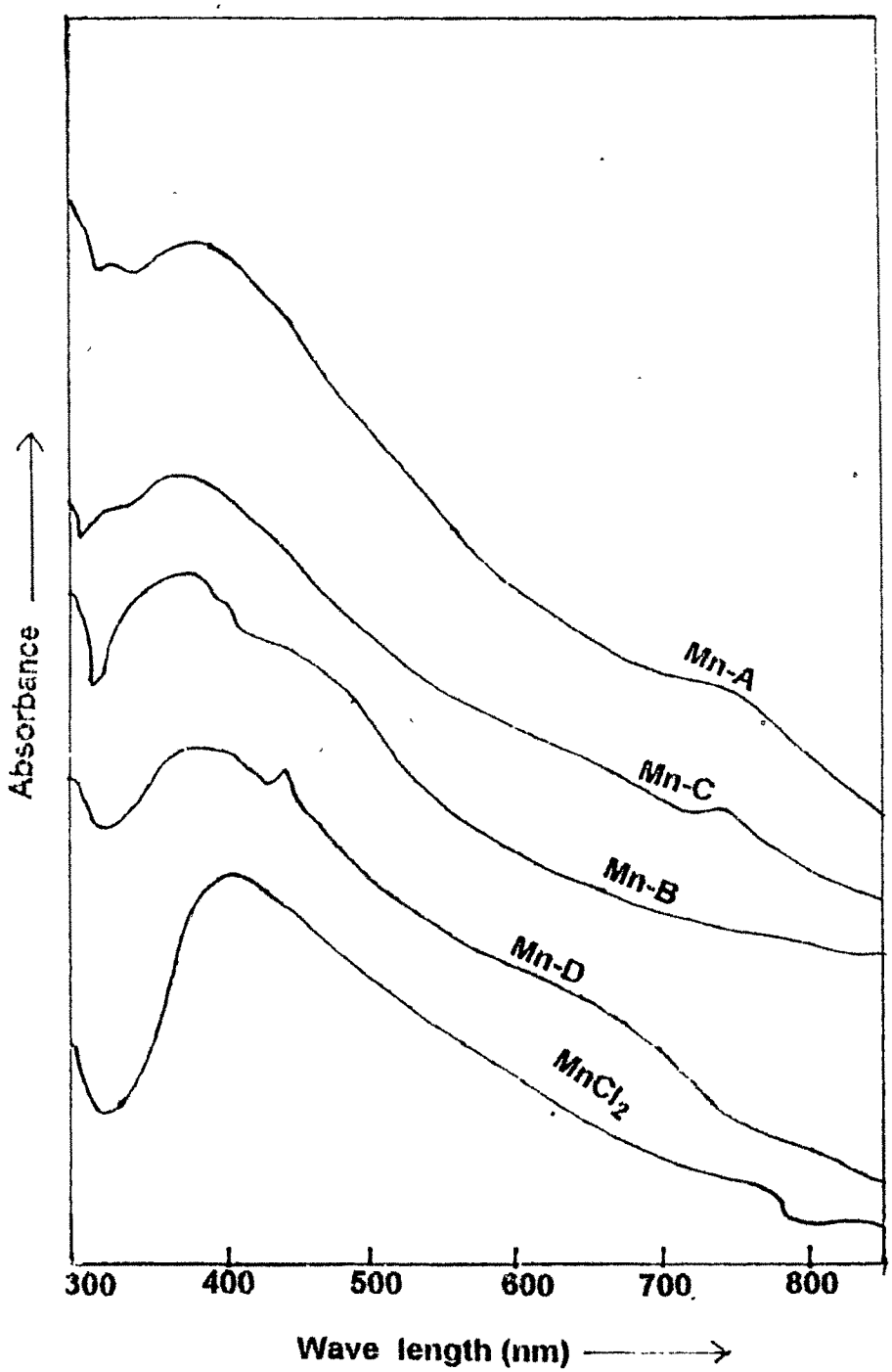


Fig 3.3 : UV-VIS spectra of Mn(II)-Schiff base complexes

atom and the coordinating atom of the ligand molecules and consequently metal-complex formation can be understood by the nature and position of absorption bands

The mid IR and far IR spectra of the polymer supported ruthenium complexes at different stages of synthesis were recorded to know the nature of coordination of the metal to the polymer **(Fig. 3.4- 3.10)** A strong band at 1639 $cm^{-1}$ is ascribed to the ν(C=N) stretching (azomethine) which in the case of Schiff base bearing polymer undergoes a downward shift with slight reduction in intensity in the supported metal catalysts This indicates coordination of the ligand nitrogen (through the azomethine "N ") to the Ru(III) metal ion which is further supported by the ν(Ru-N), ν(Ru-Cl) and ν(Ru-O) stretching vibrations which appear in the region 400-280 $cm^{-1}$ in all the catalysts [13,14] These new bands in the far IR spectra of the Ru-complexes are not seen in the starting ligands Some of the important IR spectral bands are given in **Table 3.9.**

The mid and far IR spectra of polymer supported manganese complexes at different stages of the synthesis were used to understand the nature of coordination of the metal to the polymer **(Fig. 3.11-3.14).** The spectra shows peaks in the region of 3449 $cm^{-1}$ assigned to ν(N-H) stretching frequency, that slight shift into lower wave number due to the coordination A medium intensity band at 1639 $cm^{-1}$ assigned to ν(C=N) (azomethine) indicating the formation of Schiff base on the support Weak intensity band at 500-450 $cm^{-1}$ ν(Mn-N), 720-

530 $cm^{-1}$ ν(Mn-O) and 330-290 $cm^{-1}$ ν(Mn-Cl) [15] shows the coordination of the metal with ligand to form the complex on the polymer matrix. The frequencies are compiled in **Table 3.10.**

The mid and far IR spectra of polymer supported palladium complexes at different stages of the synthesis were recorded **(Fig. 3.15-3.18)** and the IR frequencies are compiled in **Table 3.11.** From the IR spectra ν(C=N) (azomethine) band in the 1639 $cm^{-1}$ region in Schiff base liganded polymer shift to lower values (1640-1600 $cm^{-1}$) on complexation with palladium indicating "N" coordination of the ligand to the Pd(II) metal ion. The peak in the region of 3449 $cm^{-1}$ indicated to ν(N-H) stretching frequency, that slight shift into lower wave number due to the coordination. The spectra shows the weak intensity band at 530-450 $cm^{-1}$ for ν(Pd-N) , 320-300 $cm^{-1}$ for ν(Pd-Cl) and 380-320 $cm^{-1}$ for ν(Pd-O) indicating the coordination of metal with ligand to form the complex on polymer support [15].

### 3.1.4 MORPHOLOGY OF THE POLYMER SUPPORTS AND POLYMER BOUND CATALYSTS (SEM)

This technique allows essentially the imaging of the topography of a solid surface by use of back scattered or secondary electrons [16] The scanning electron microscope is especially designed for the study of bulk samples. The low energy electrons (secondary electron) provide topographical contrast,

**Table 3.9**
**I.R. spectral data of poly(styrene-divinylbenzene)-Schiff bases and their Ru(III) Complexes**

| Compound | ν(N-H) $cm^{-1}$ | ν(C=N) $cm^{-1}$ | ν(Ru-O) $cm^{-1}$ | ν(Ru-N) $cm^{-1}$ | ν(Ru-Cl) $cm^{-1}$ |
|---|---|---|---|---|---|
| 5% P(S-DVB)(1,3-dap-SB) | $3449_{br}$ | $1633_{s}$ | | | |
| 8% P(S-DVB)(1,3-dap-SB) | $3432_{br}$ | $1639_{s}$ | | | |
| 5% P(S-DVB)(4,4'-dabp-SB) | $3407_{br}$ | $1614_{s}$ | | | |
| 8% P(S-DVB)(4,4'-dabp-SB) | $3409_{br}$ | $1638_{s}$ | | | |
| **Ru-A** | $3429_{br}$ | $1638_{s}$ | 424 | 384 | 282 |
| **Ru-B** | $3409_{br}$ | $1606_{s}$ | 431 | 383 | 302 |
| **Ru-C** | $3443_{br}$ | $1639_{s}$ | 434 | 389 | 296 |
| **Ru-D** | $3409_{br}$ | $1613_{s}$ | 430 | 378 | 287 |

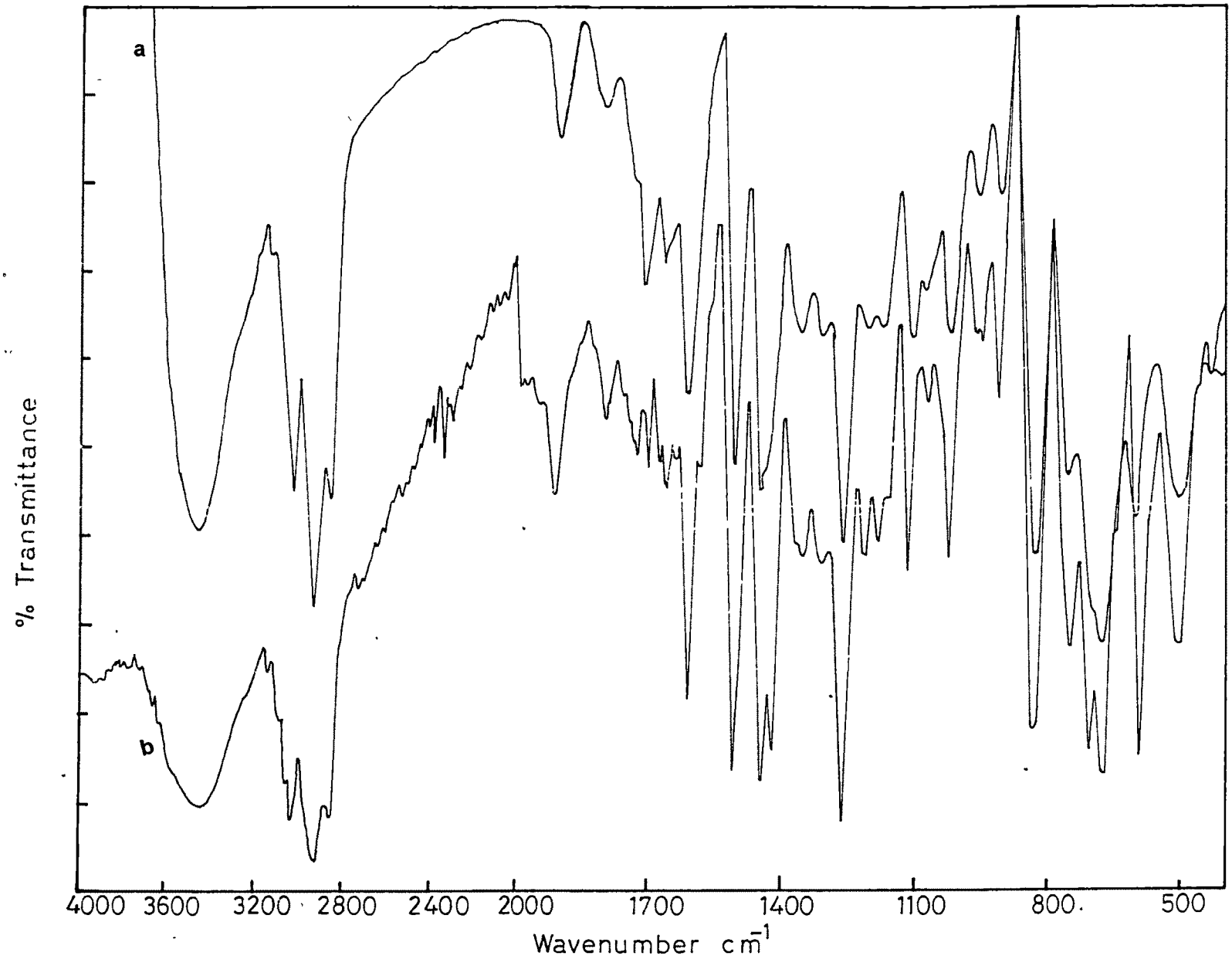


**Fig. 3.4 I. R. Spectra of (a) 5% P(S-DVB)$CH_2Cl$ (b) 8% P(S-DVB)$CH_2Cl$**

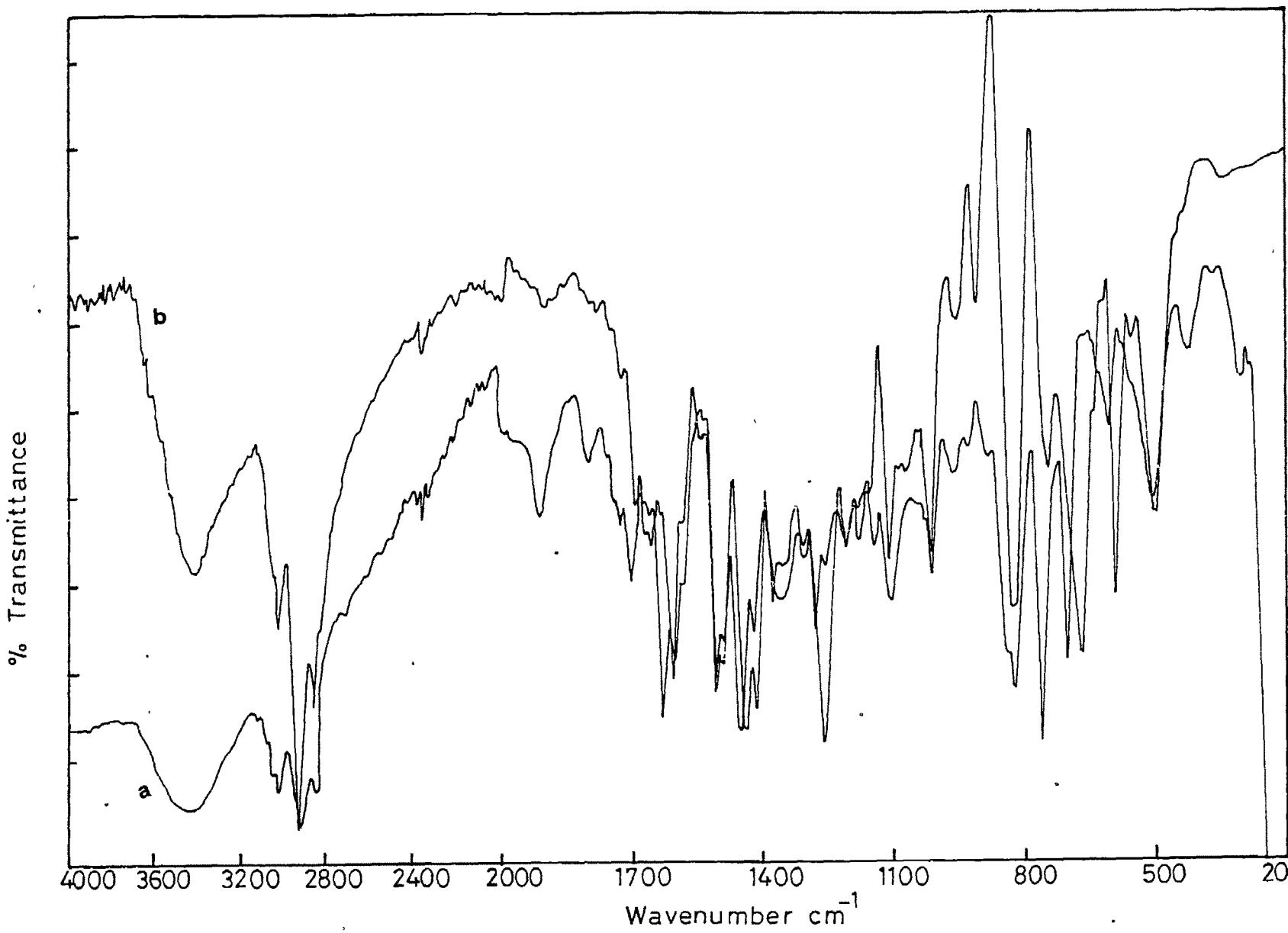


**Fig. 3.5 I. R. Spectra of (a) P(S-DVB) 1,3-dap (b) P(S-DVB) (1,3-dap-SB)**

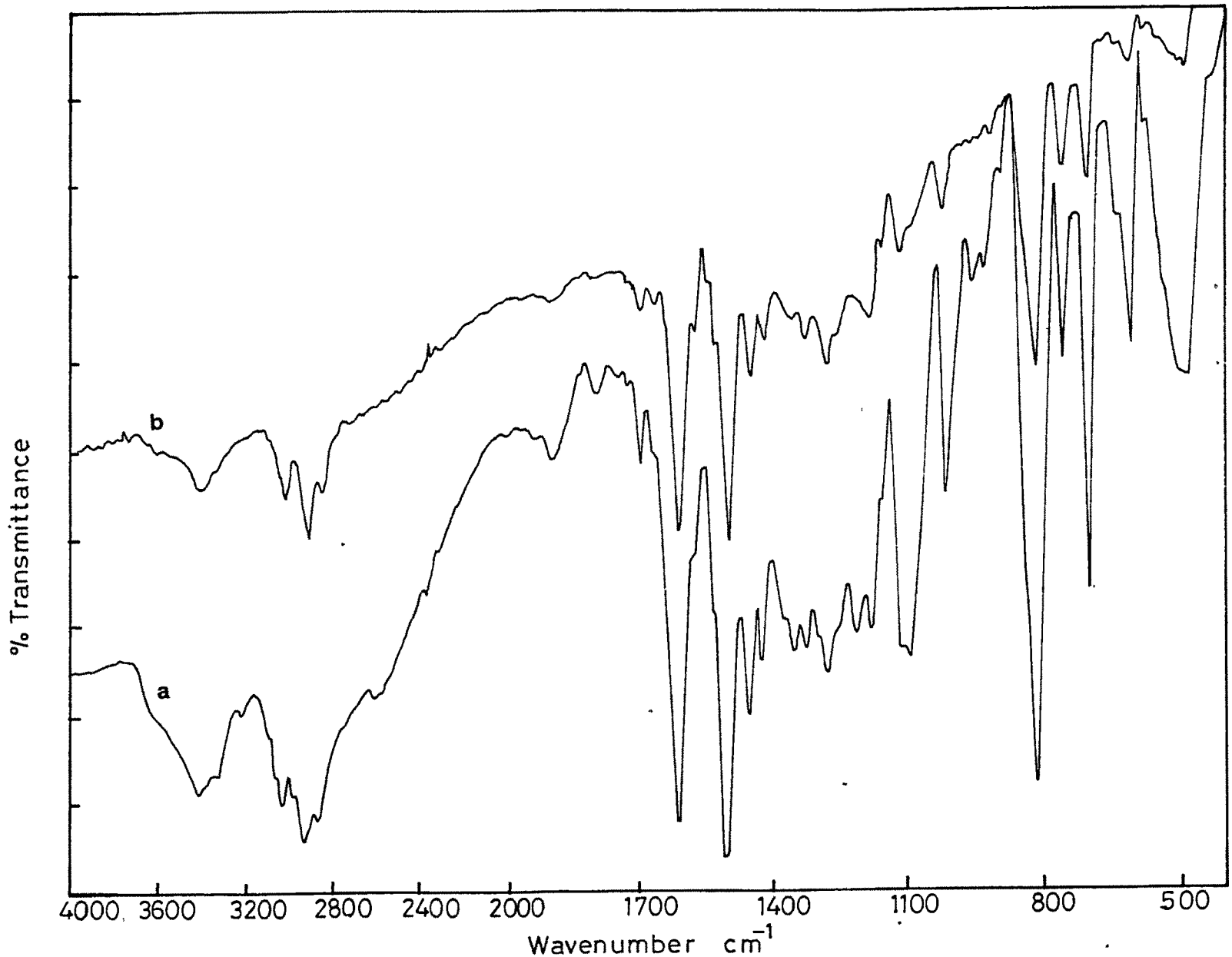


**Fig. 3.6 I. R. Spectra of (a) P(S-DVB) 4,4'-dabp (b) P(S-DVB) (4,4'-dabp-SB)**

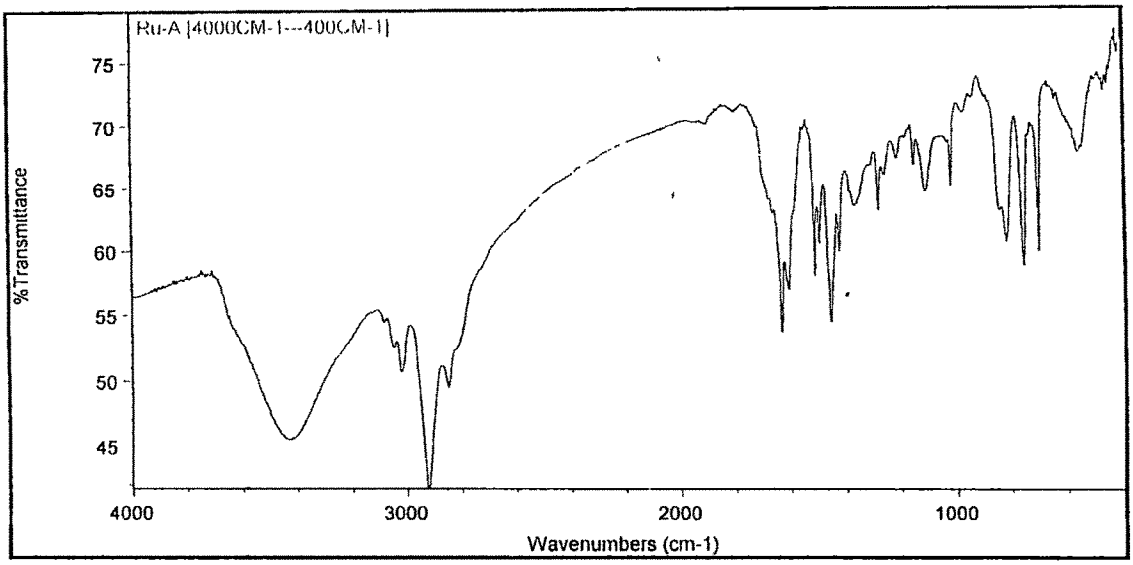


**Fig : 3.7 (a) : I.R.Spectra of 5% P(S-DVB) Ru (III) (DAP - SB) [ Ru-A]**

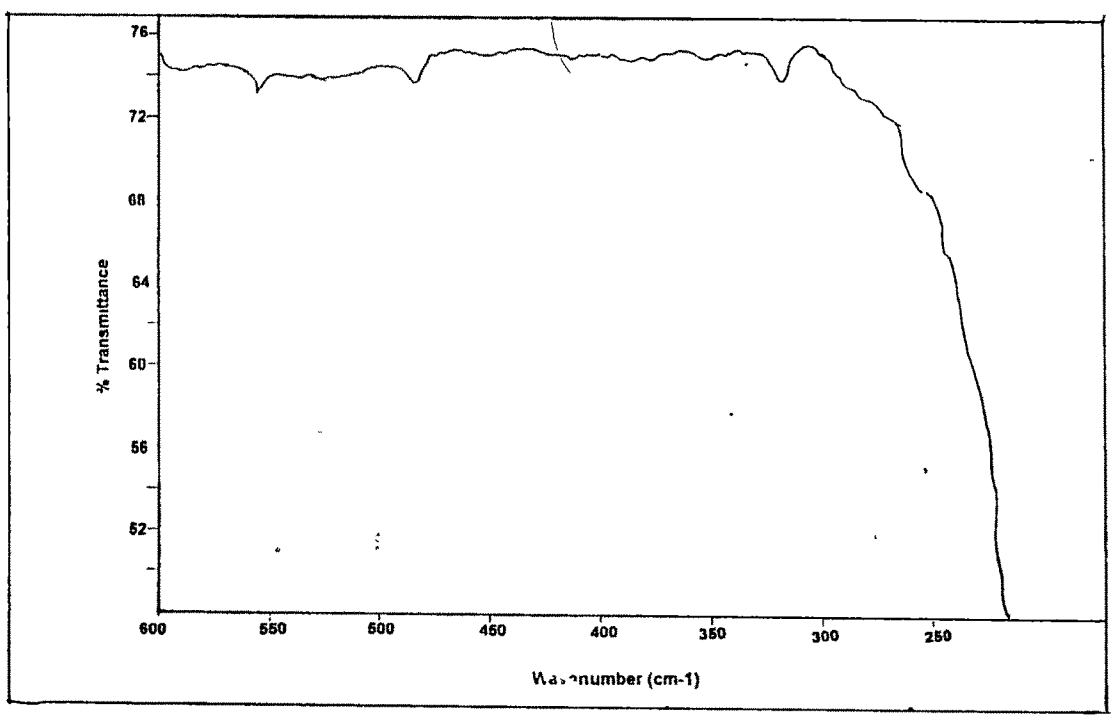


**Fig : 3.7 (b) : I.R.Spectra of 5% P(S-DVB) Ru (III) (DAP - SB) [ Ru-A] [500 – 200 $cm^{-1}$]**

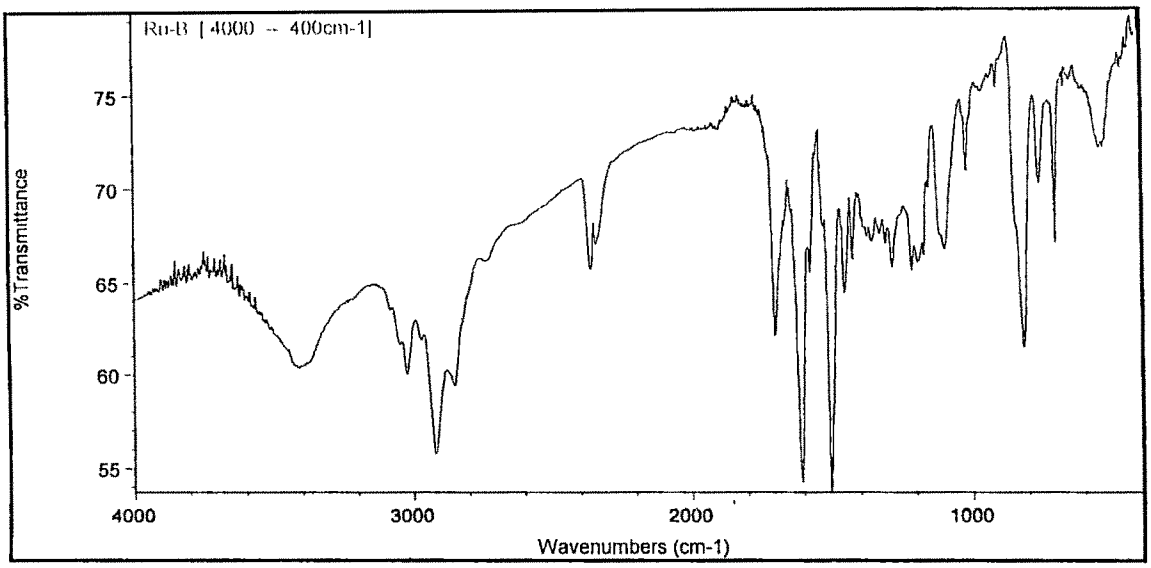


**Fig : 3.8 (a) : I.R.Spectra of 8% P(S-DVB) Ru (III) (DAP - SB) [ Ru-B]**

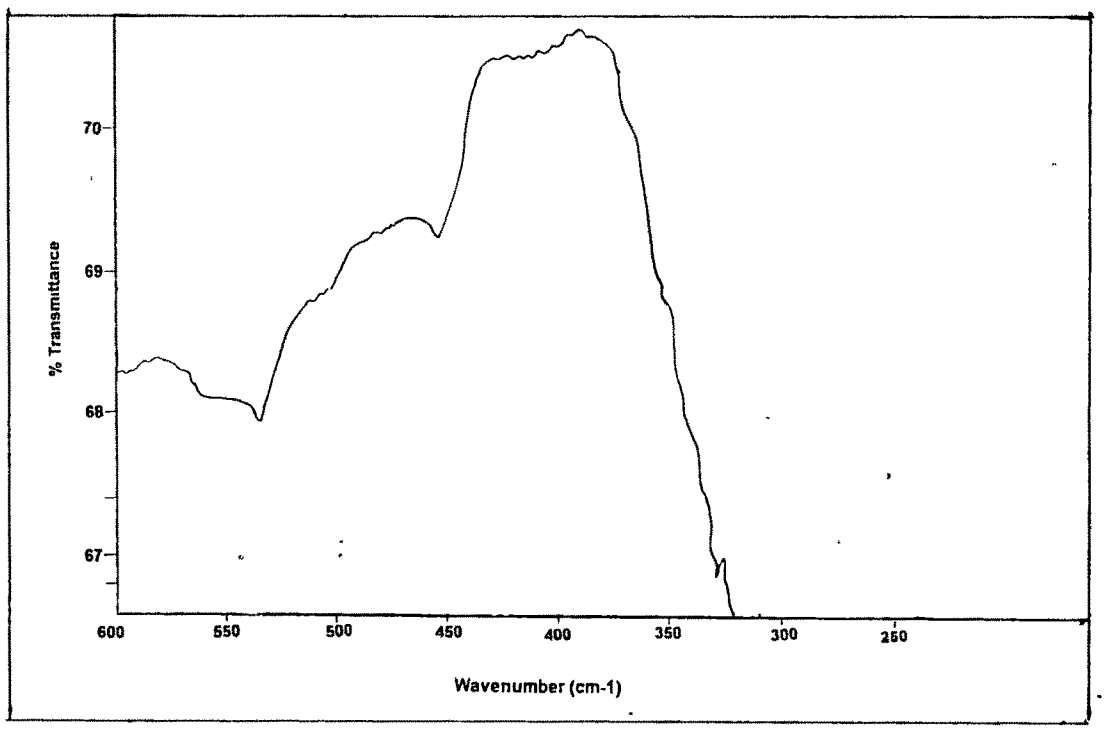


**Fig : 3.8 (b) : I.R.Spectra of 8% P(S-DVB) Ru (III) (DAP - SB) [ Ru-B] [500 – 200cm$^{-1}$]**

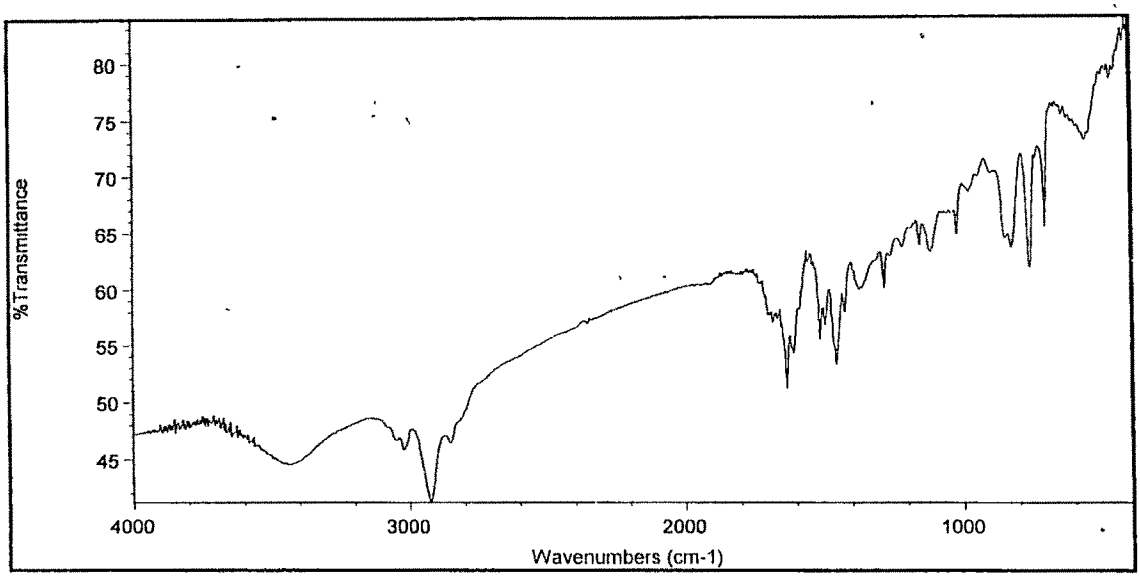


**Fig : 3.9 (a) : I.R.Spectra of 5% P(S-DVB) Ru(III) (DABP - SB) [ Ru-C]**

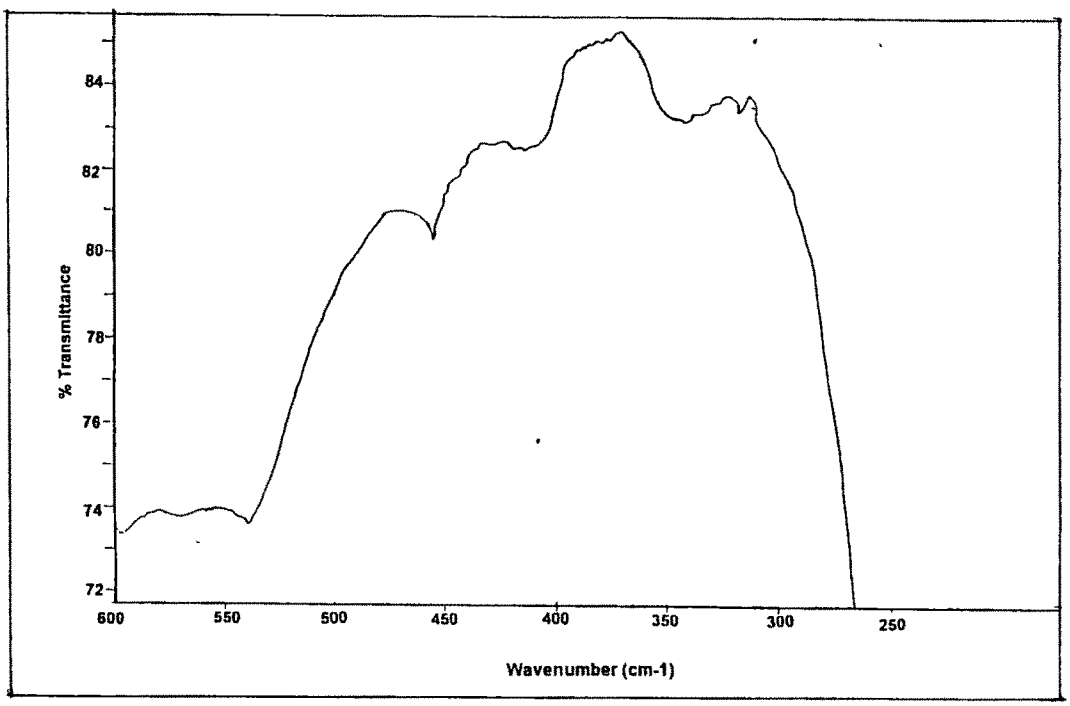


**Fig : 3.9 (b): I.R.Spectra of 5% P(S-DVB) Ru(III) (DABP - SB) [ Ru-C] [500 – 200 $cm^{-1}$]**

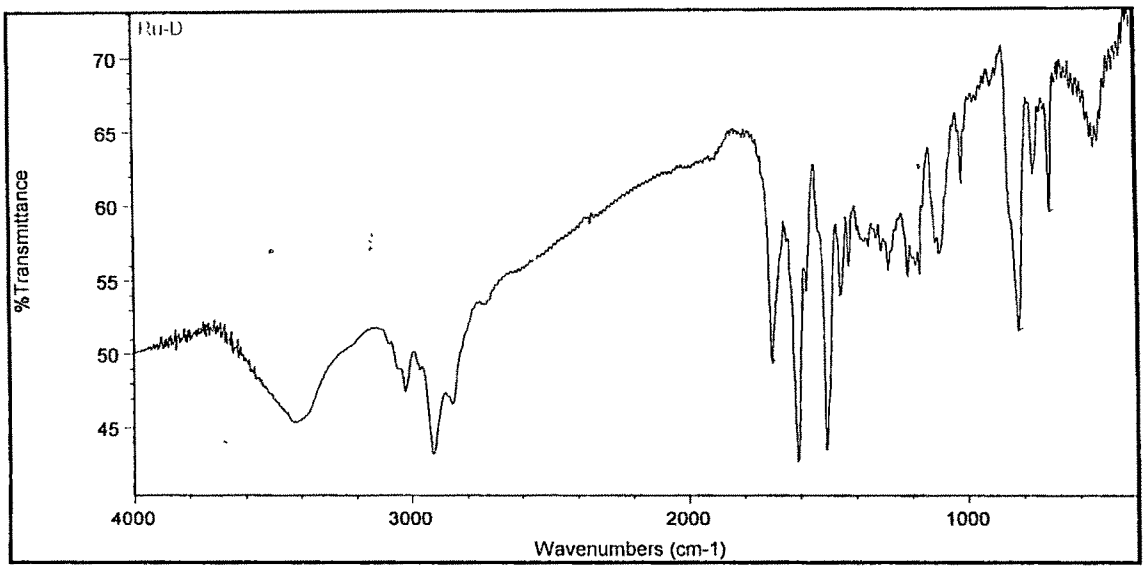


**Fig : 3.10(a) :I.R.Spectra of 8% P(S-DVB) Ru(III) (DABP - SB) . [ Ru-D]**

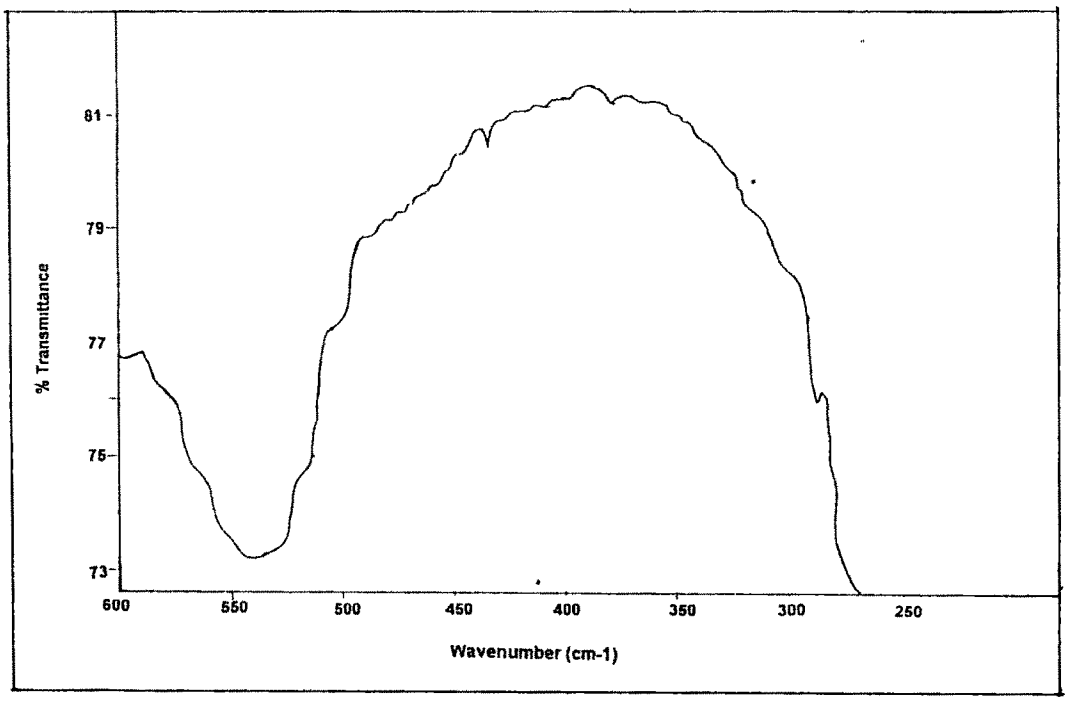


**Fig :3.10(b) :I.R.Spectra of 8% P(S-DVB) Ru(III) (DABP - SB) [ Ru-D] [500 – 200 $cm^{-1}$]**

**Table 3.10**
**I.R. spectral data of poly(styrene-divinylbenzene)-Schiff bases and their Mn (II) Complexes**

| Compound | ν(N-H) $cm^{-1}$ | ν(C=N) $cm^{-1}$ | ν(Mn-O) $cm^{-1}$ | ν(Mn-N) $cm^{-1}$ | ν(Mn-Cl) $cm^{-1}$ |
|---|---|---|---|---|---|
| 5% P(S-DVB)(1,3-dap-SB) | $3449_{br}$ | $1633_s$ | | | |
| 8% P(S-DVB)(1,3-dap-SB) | $3432_{br}$ | $1639_s$ | | | |
| 5%P(S-DVB)(4,4'-dabp-SB) | $3407_{br}$ | $1614_s$ | | | |
| 8% P(S-DVB)(4,4-dabp-SB) | $3409_{br}$ | $1638_s$ | | | |
| **Mn-A** | $3443_{br}$ | $1633_s$ | 540 | 453 | 327 |
| **Mn-B** | $3416_{br}$ | $1613_s$ | 552 | 486 | 317 |
| **Mn-C** | $3436_{br}$ | $1606_s$ | 540 | 455 | 316 |
| **Mn-D** | $3429_{br}$ | $1639_s$ | 545 | 451 | 320 |

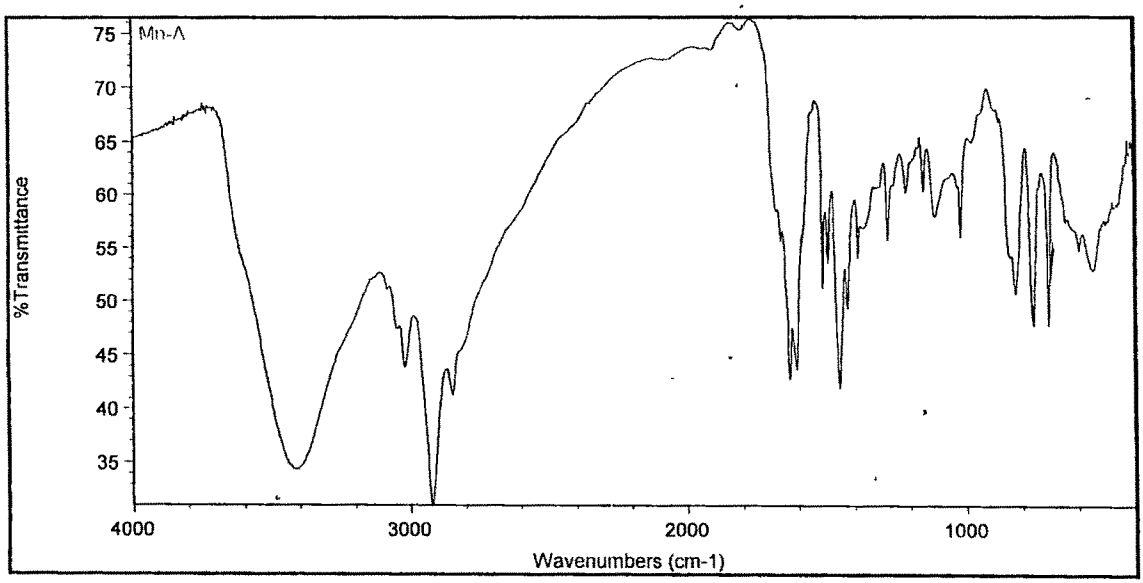


**Fig : 3.11 (a) : I.R.Spectra of 5% P(S-DVB) Mn(II) (DAP - SB) [ Mn-A]**

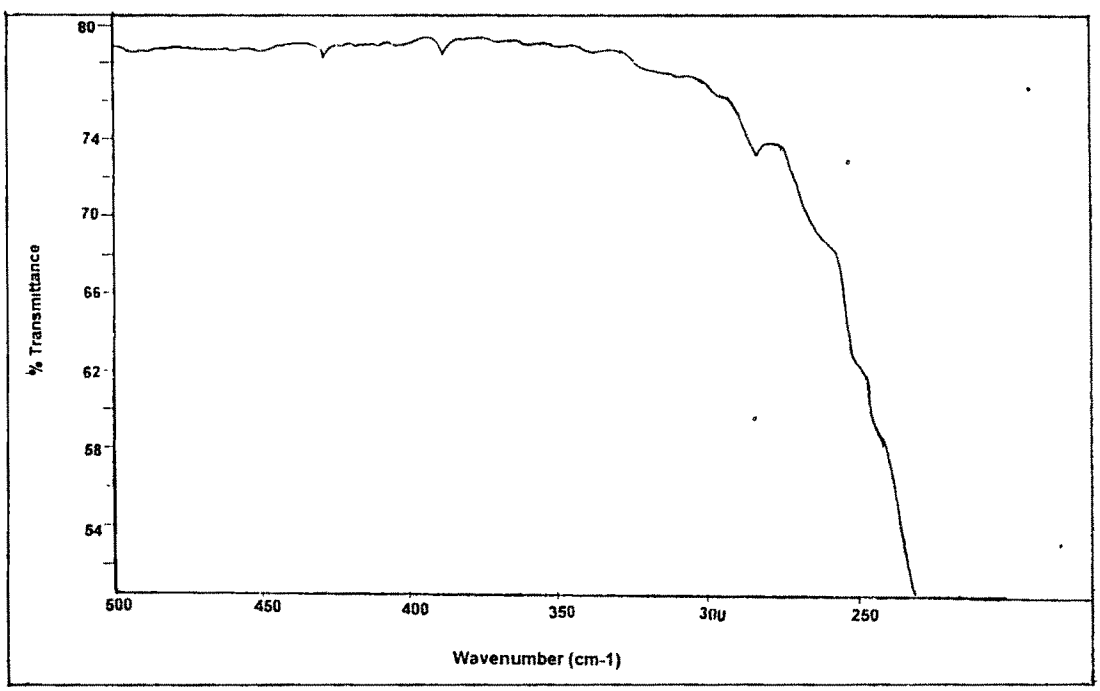


**Fig : 3.11 (b) : I.R.Spectra of 5% P(S-DVB) Mn(II) (DAP - SB) [ Mn-A] [500 – 200 $cm^{-1}$]**

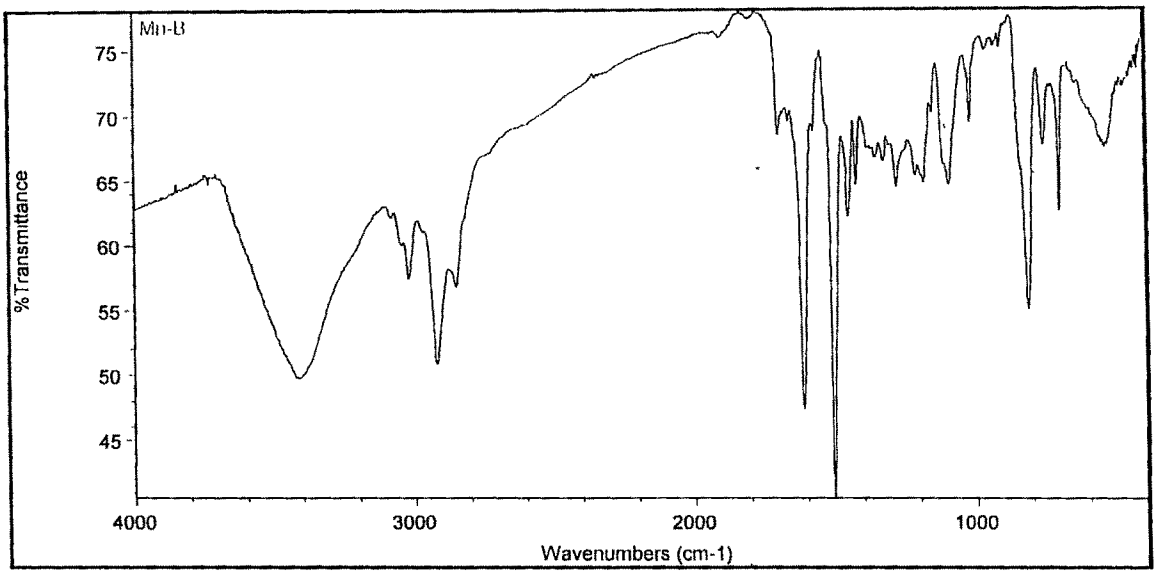


**Fig : 3.12 (a) : I.R.Spectra of 8% P(S-DVB) Mn(II) (DAP - SB) [ Mn-B]**

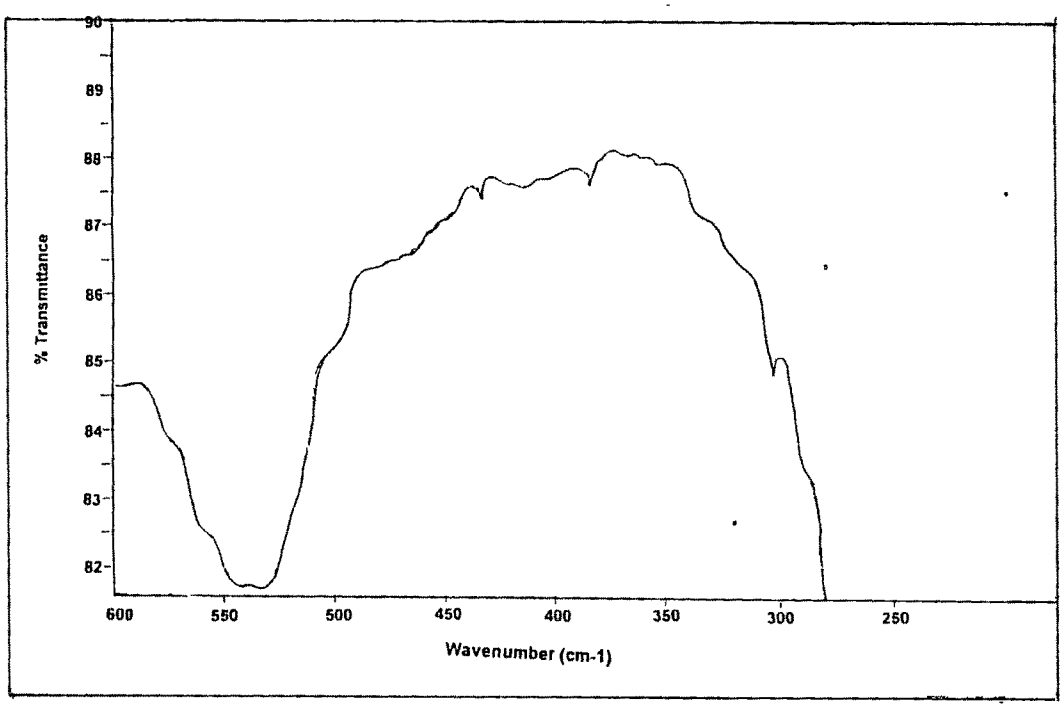


**Fig : 3.12 (b) : I.R.Spectra of 8% P(S-DVB) Mn(II) (DAP - SB) [ Mn-B] [500 – 200 $cm^{-1}$]**

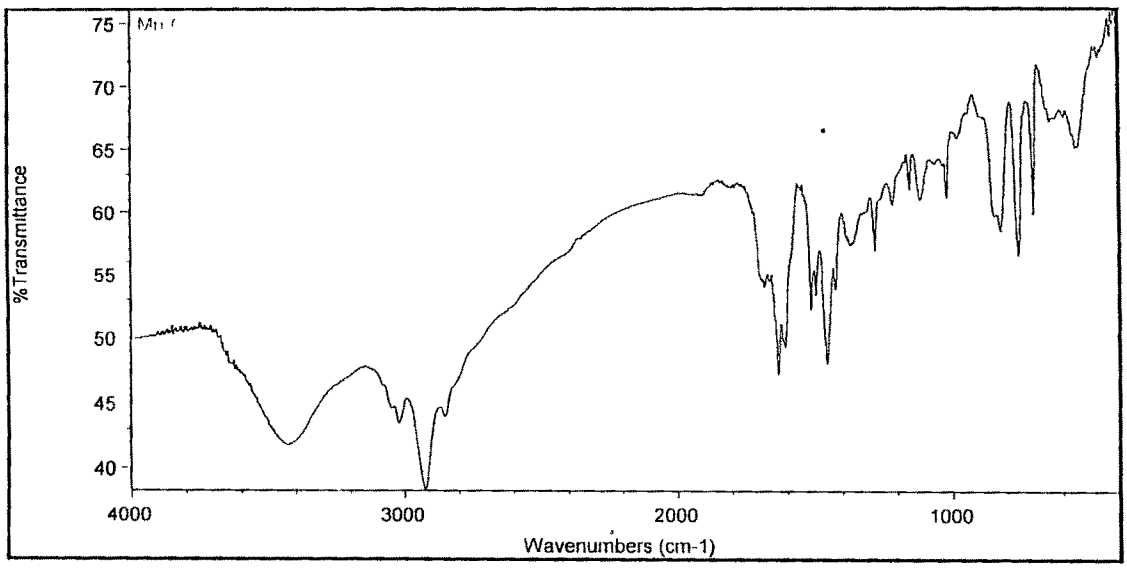


**Fig. 3.13(a) : I.R. Spectra of 5% P(S-DVB) Mn(II) (DABP-SB) [ Mn- C]**

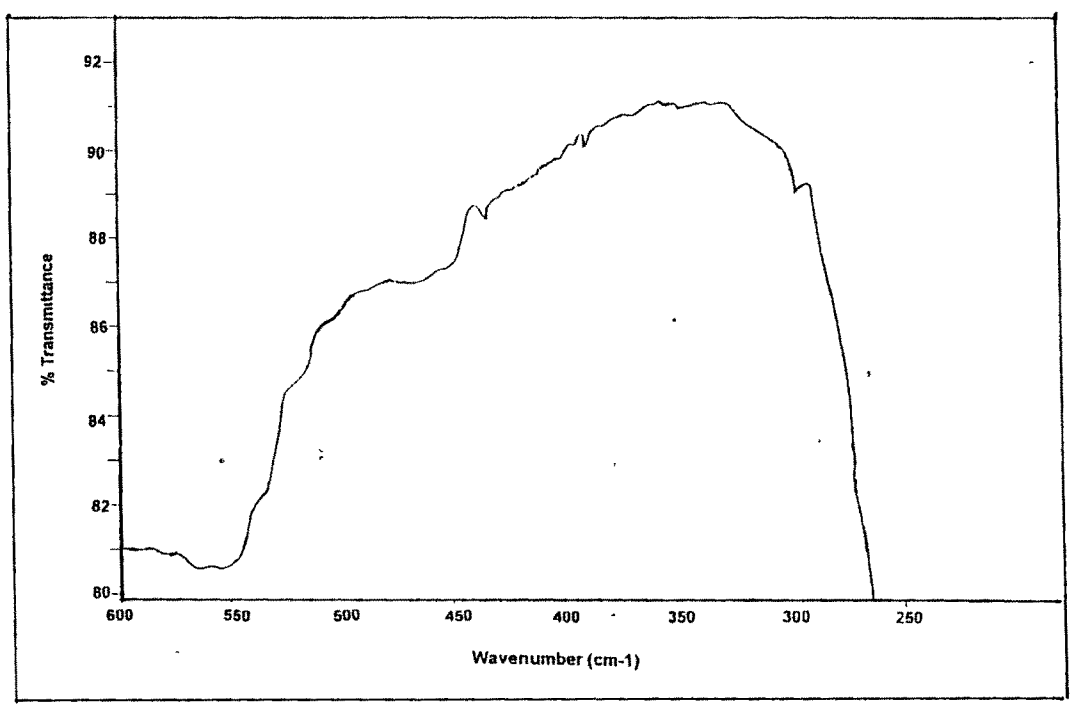


**Fig. 3.13 (b) : I.R. Spectra of 5% P(S-DVB) Mn(II) (DABP-SB) [ Mn- C] [500 – 200 $cm^{-1}$]**

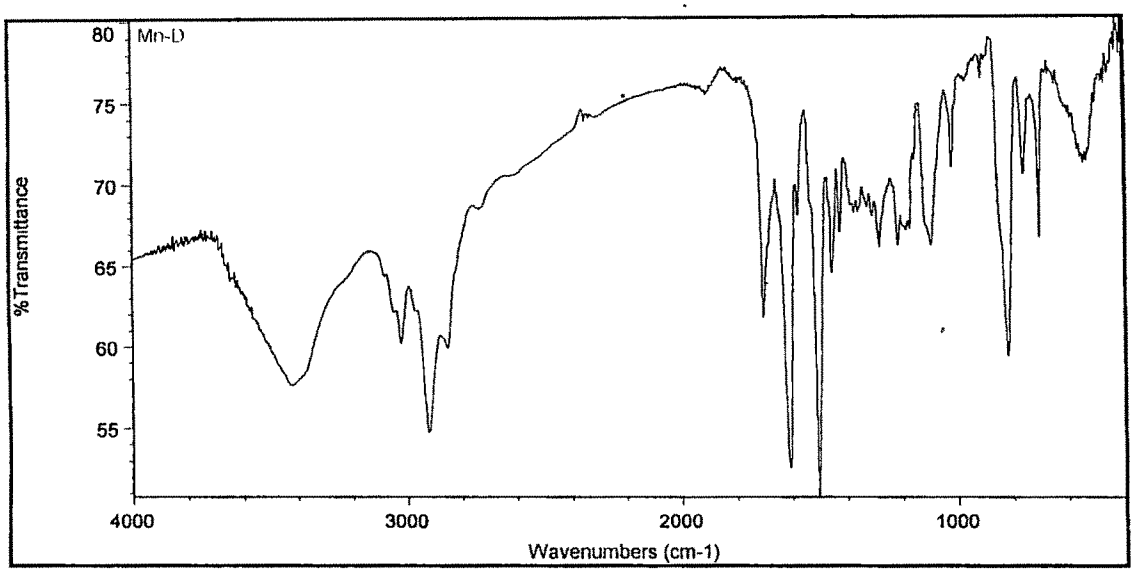


**Fig : 3.14(a) :I.R.Spectra of 8% P(S-DVB) Mn(II) (DABP - SB) [ Mn-D]**

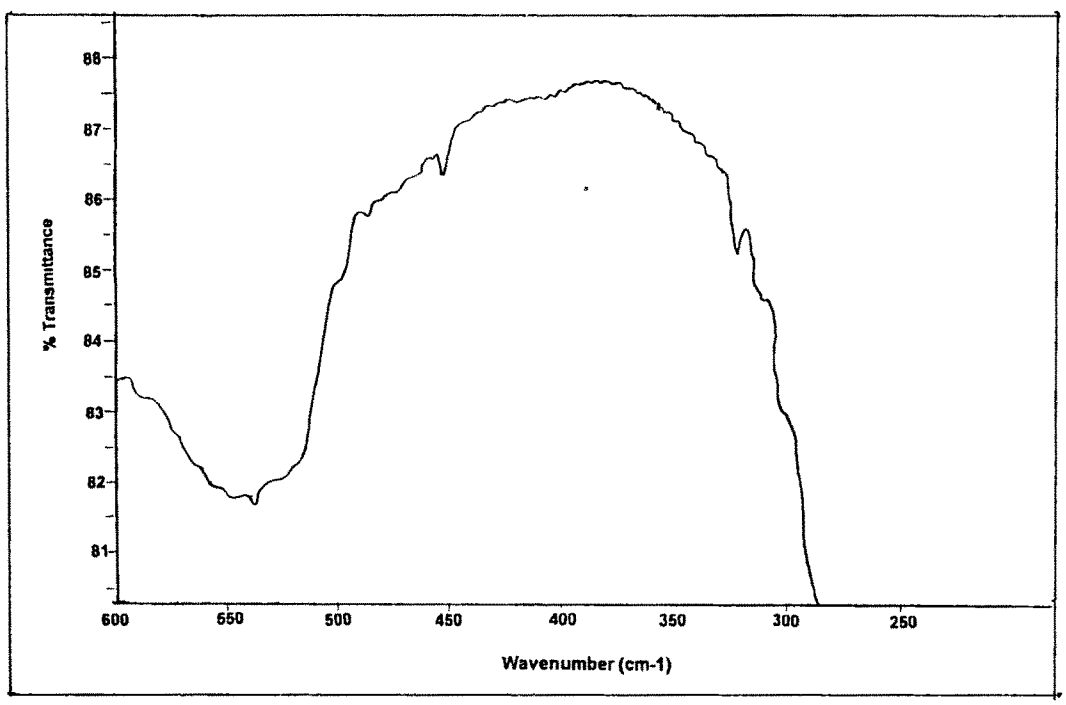


**Fig : 3.14(b) : I.R.Spectra of 8% P(S-DVB) Mn(II) (DABP - SB) [ Mn-D] [500 – 200 $cm^{-1}$]**

**Table 3.11**
**I.R. spectral data of poly(styrene-divinylbenzene)-Schiff bases and their Pd(II) Complexes**

| Compound | ν(N-H) $cm^{-1}$ | ν(C=N) $cm^{-1}$ | ν(Pd-O) $cm^{-1}$ | ν(Pd-N) $cm^{-1}$ | ν(Pd-Cl) $cm^{-1}$ |
|---|---|---|---|---|---|
| 5% P(S-DVB)(1,3-dap-SB) | $3449_{br}$ | $1633_{s}$ | | | |
| 8% P(S-DVB)(1,3-dap-SB) | $3432_{br}$ | $1639_{s}$ | | | |
| 5%P(S-DVB)(4,4'-dabp-SB) | $3407_{br}$ | $1614_{s}$ | | | |
| 8%P(S-DVB)(4,4'-dabp-SB) | $3409_{br}$ | $1638_{s}$ | | | |
| **Pd-A** | $3436_{br}$ | $1633_{s}$ | 320 | 485 | 302 |
| **Pd-B** | $3409_{br}$ | $1606_{s}$ | 354 | 479 | 303 |
| **Pd-C** | $3429_{br}$ | $1633_{s}$ | 350 | 462 | 302 |
| **Pd-D** | $3430_{br}$ | $1600_{s}$ | 375 | 456 | 302 |

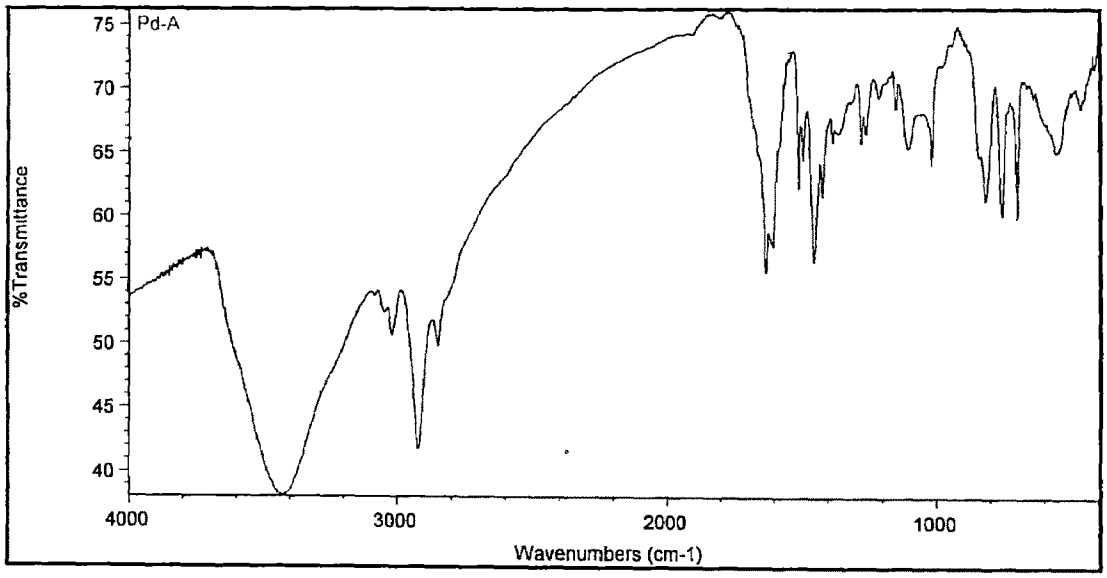


**Fig : 3.15 (a) : I.R.Spectra of 5% P(S-DVB) Pd(II) (DAP - SB) [ Pd-A]**

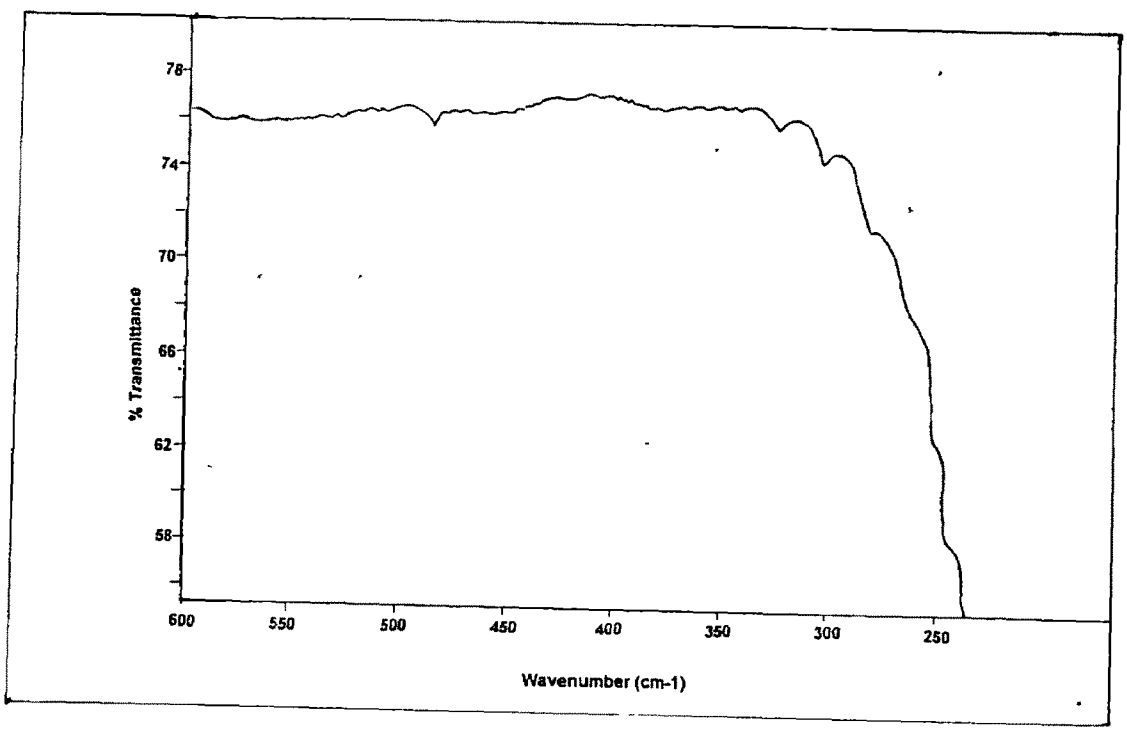


**Fig : 3.15 (b) : I.R.Spectra of 5% P(S-DVB) Pd(II) (DAP - SB) [ Pd-A] [500 – 200 $cm^{-1}$]**

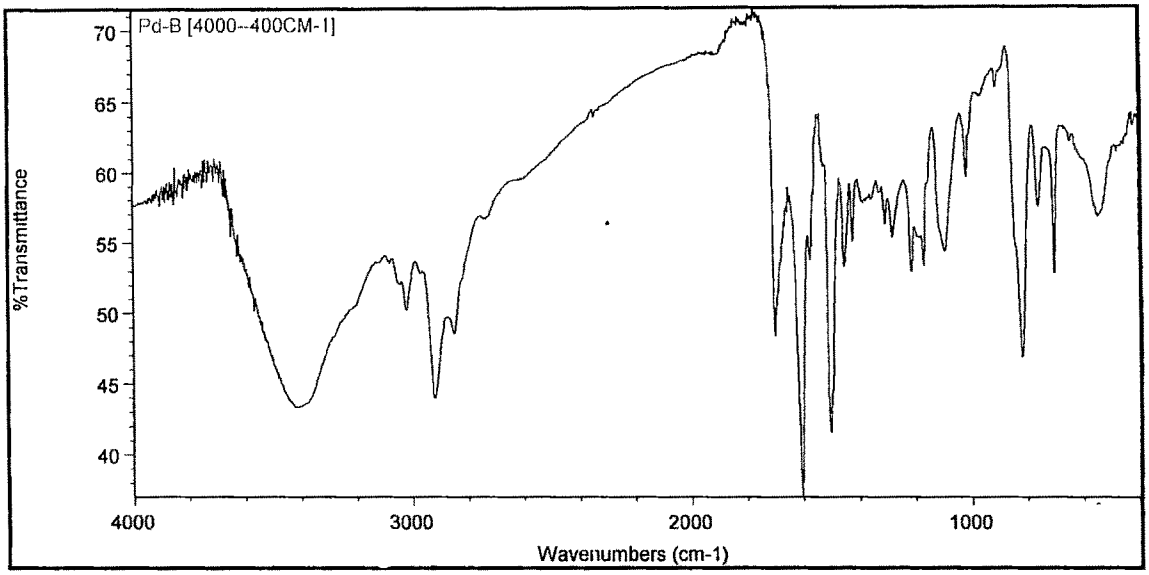


**Fig : 3.16 (a) : I.R.Spectra of 8% P(S-DVB) Pd(II) (DAP - SB) [ Pd-B]**

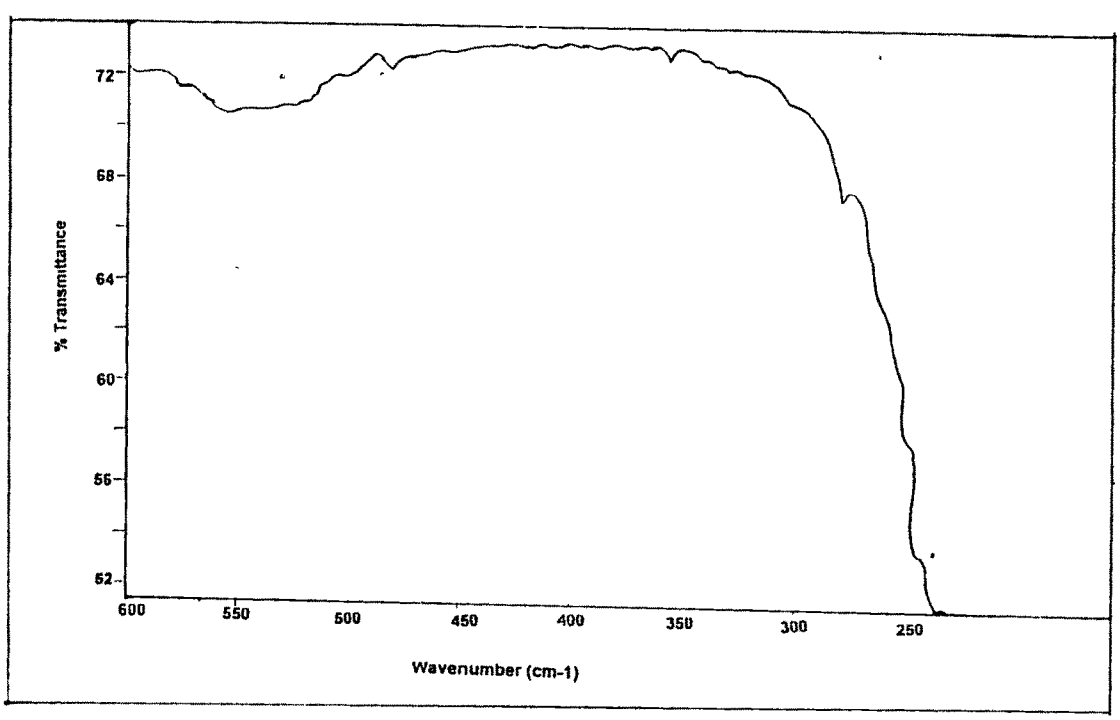


**Fig : 3.16 (b) : I.R.Spectra of 8% P(S-DVB) Pd(II) (DAP - SB) [ Pd-B] [500 – 200 $cm^{-1}$]**

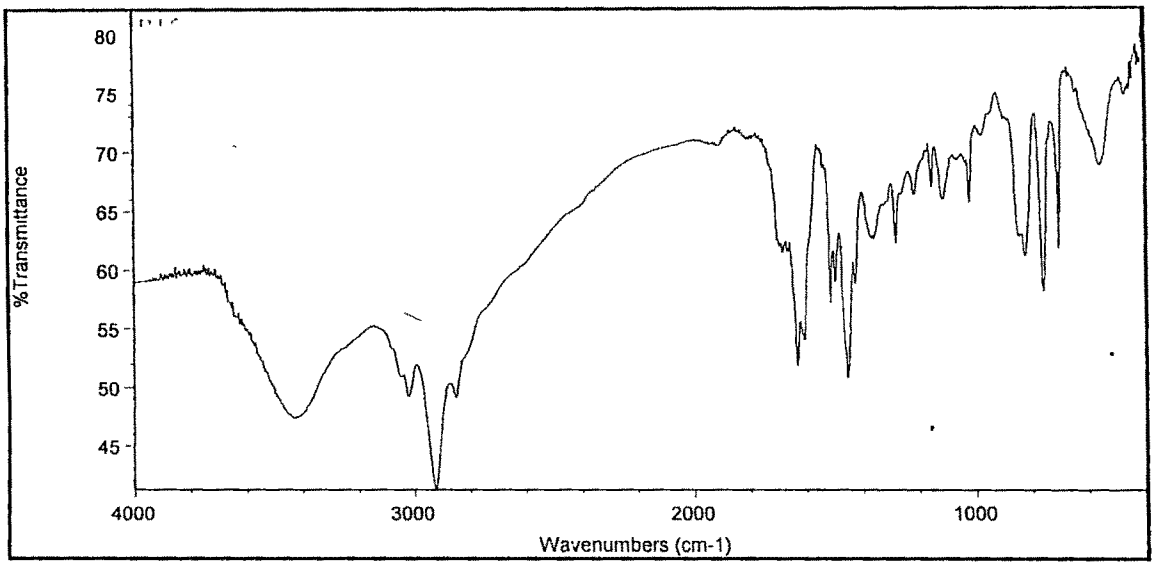


**Fig : 3.17(a) : I.R.Spectra of 5% P(S-DVB) Pd(II) (DABP - SB) [ Pd-C]**

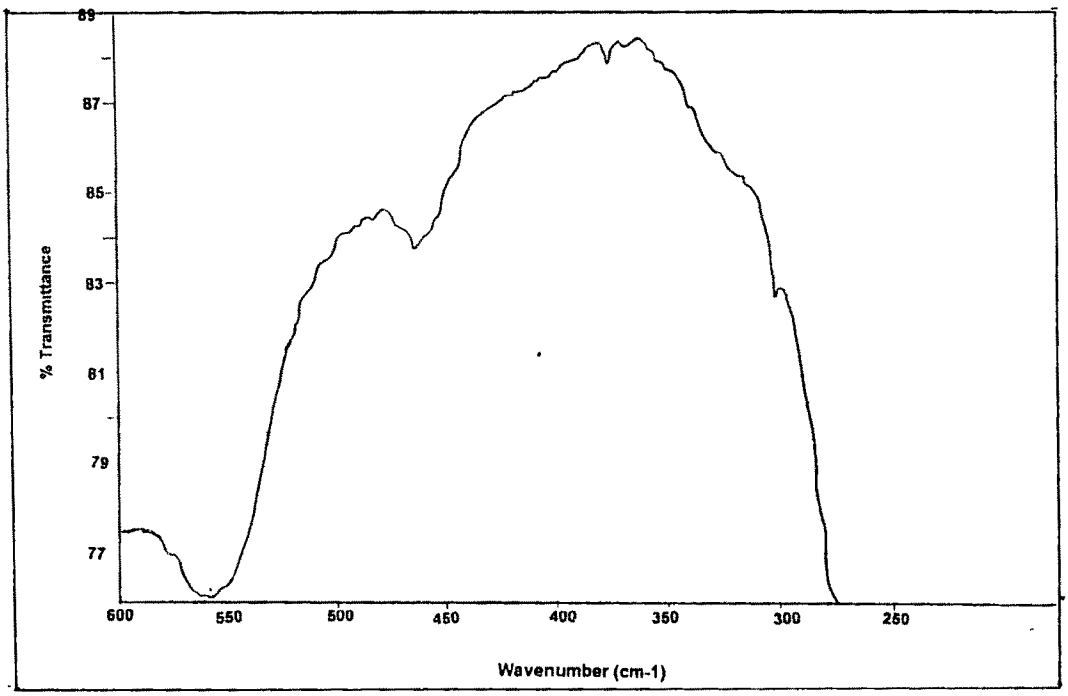


**Fig :3.17 (b) :I.R.Spectra of 5% P(S-DVB) Pd(II) (DABP - SB) [ Pd-C] [500 – 200 $cm^{-1}$]**

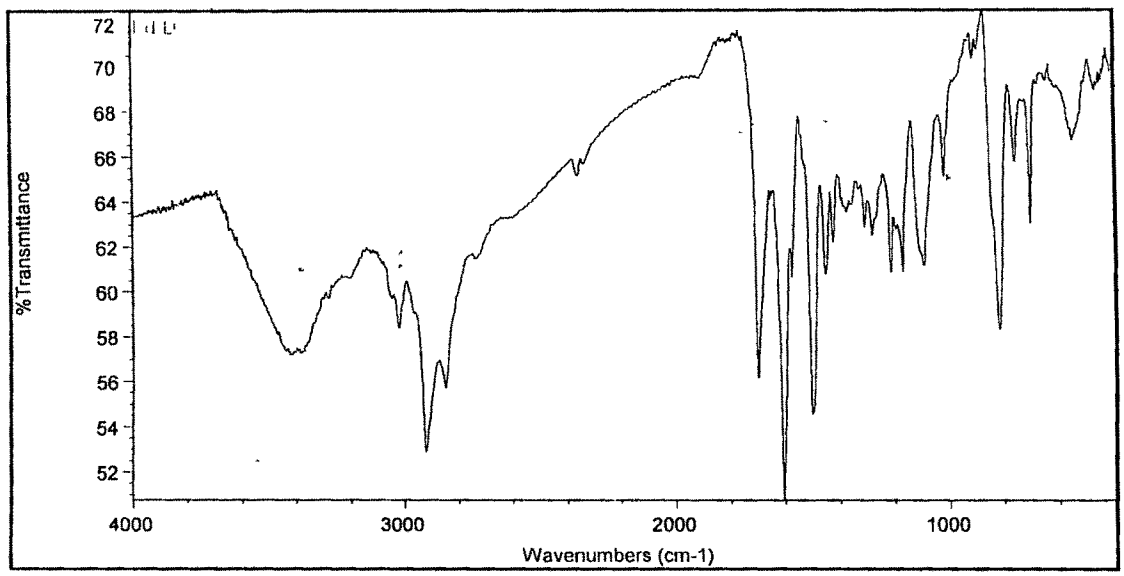


**Fig : 3.18 (a) : I.R.Spectra of 8% P(S-DVB) Pd(II) (DABP - SB) [ Pd-D]**

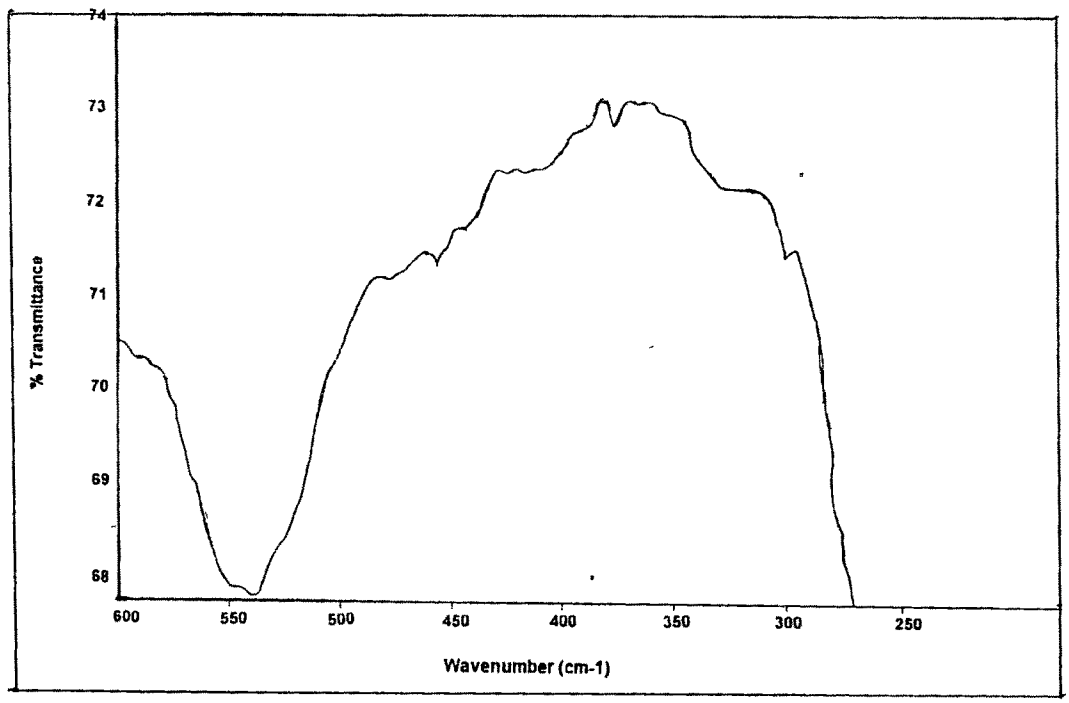


**Fig : 3.18 (b) : I.R.Spectra of 8% P(S-DVB) Pd(II) (DABP - SB) [ Pd-D] [500 – 200 $cm^{-1}$]**

allowing study of the relief of the surface The behaviour of a catalyst depends upon the structure and composition of the active component as well as morphology of its supporting medium It can be determined on the basis of its structure at a range of magnification (from a few hundred to a few million times) which gives the information about the nature and the distribution of the active components, the nature of the porosity etc. The magnification in a simple electron microscopy is limited and extension of magnification by several orders of magnitude is obtained with SEM The morphology of the catalyst can be studied with this technique [17]

Scanning electron micrographs (SEM) at various stages of preparation of the polymer supported catalysts were recorded to understand morphological changes occurring on the surface of the polymer Scanning was done 50-100 μ range across the length of the polymer beads Comparison of images taken at different magnification showed that the smooth and flat surface of the starting poly (S-DVB) is distinctly altered, exhibiting considerable roughening of the top layer after functionalization Representative SEM micrographs are shown in **Plate 3.1-3.4.** Apparently, low loading seem to limit further surface characterization.

### 3.1.7 THERMAL STABILITY OF SUPPORTS AND CATALYSTS

Thermoanalytical techniques are among the most important and widely used methods for the characterization of the properties and reactivities of the

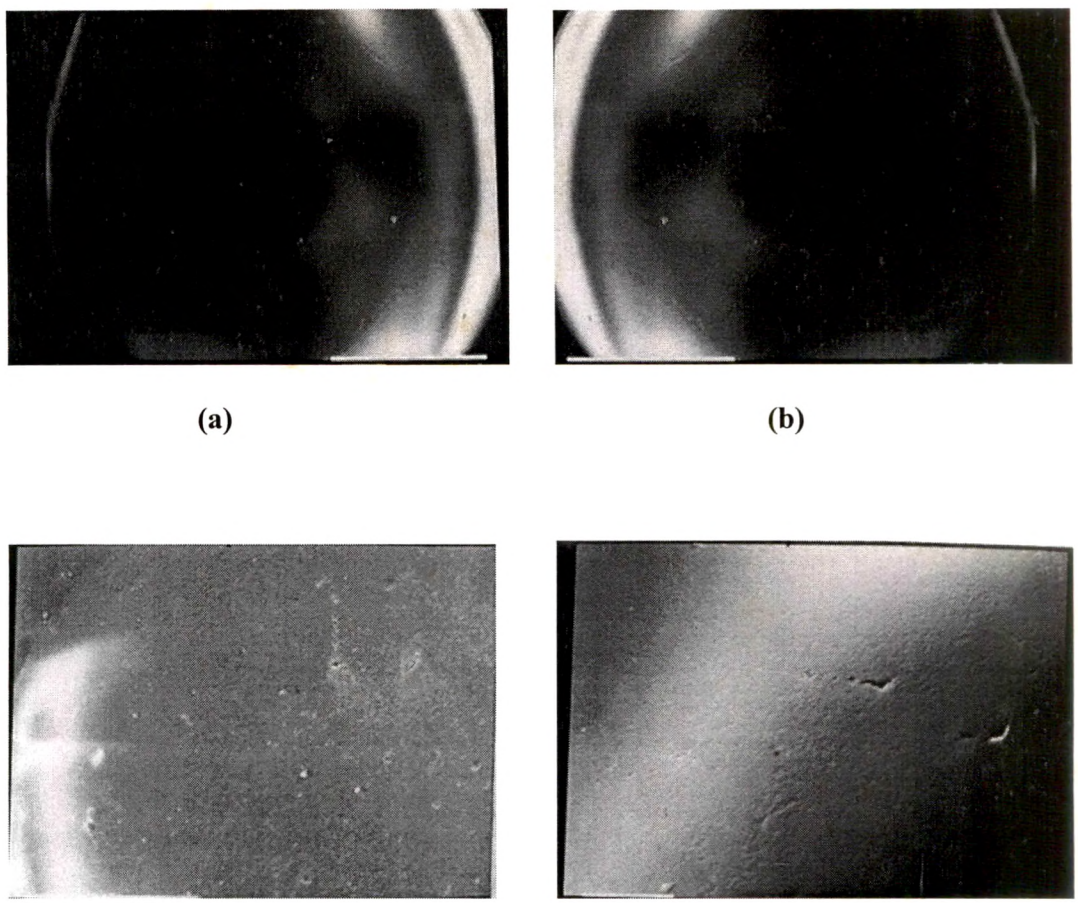

**Plate 3.1 Scanning electron micrographs of (a) 5% P(S-DVB) (b) 8% P(S-DVB) (c) P(S-DVB) (1,3-dap-SB) (d) P(S-DVB) (4,4'-dabp-SB)**

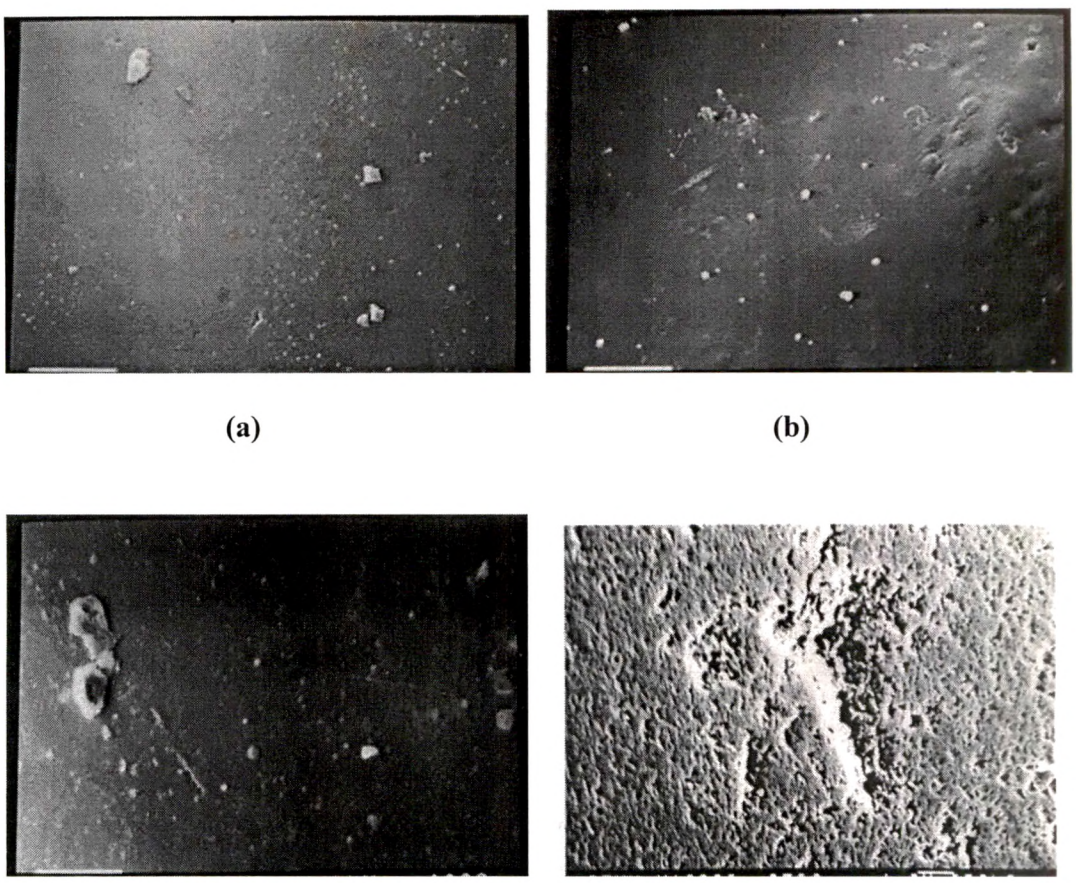

**Plate 3.2 Scanning electron micrographs of (a) Ru-A (b) Ru-B (c) Ru-C (d) Ru-D**

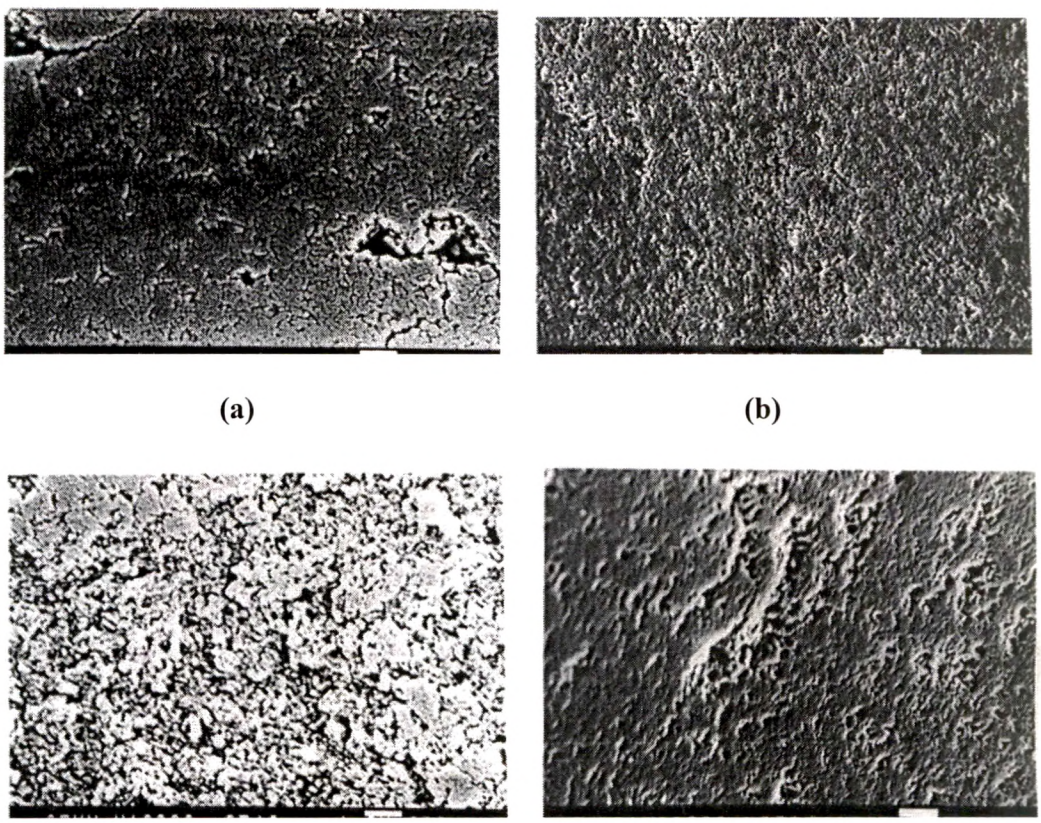

**Plate 3.3 Scanning electron micrographs of (a) Mn-A (b) Mn-B (c) Mn-C (d) Mn-D**

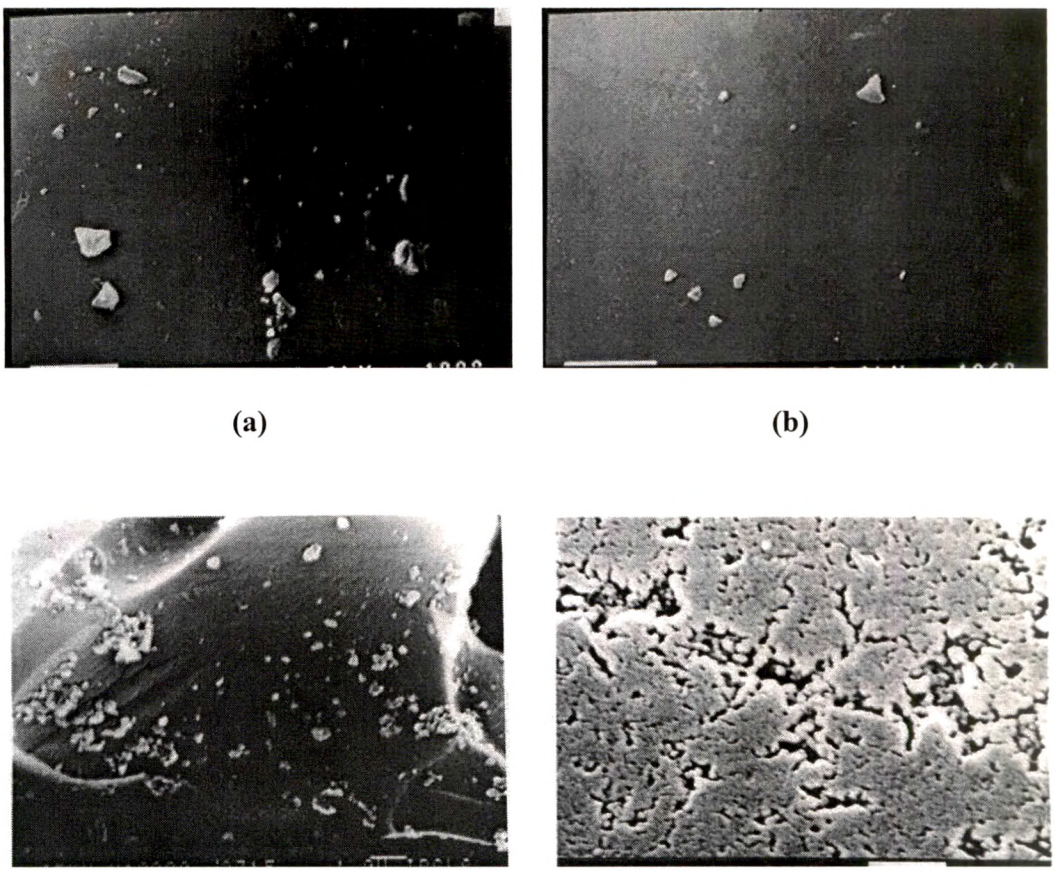

**Plate 3.4 Scanning electron micrographs of (a) Pd-A (b) Pd-B (c) Pd-C (d) Pd-D**

solid catalyst These techniques involve the measurements of the response of the catalyst under study (e g energy or mass released or consumed) as the temperature is changed Most techniques are carried out dynamically by application of a linear temperature program Differential thermal analysis (DTA), thermogravimetry (TG) and differential scanning calorimetry (DSC) are standard techniques in solid state chemistry [18,19] The catalytic chemist will use these techniques to study the genesis of catalytic materials via solid state reactions

A degradation in the TG was observed for the unsupported polymer in the 430-480°C temperature range On the other hand all the (Ru, Mn and Pd) supported catalysts degrade at considerably lower temperature range **(Table 3.12 to 3.14).** Some weight loss (2%) was observed at ~110 °C due to loosely bound surface moisture or volatiles on the surface of catalysts The lower stability of the metal supported polymer is also revealed by higher weight loss which may be due to dissociation of the Schiff base ligand moieties from the catalyst Typical thermograms are shown in **Fig. 3.19-3.22.** Due to hazards associated with hydroperoxide in oxidation reaction, the preferred working temperature were deliberately maintained below 70 °C

**Table 3.12**
**Thermoanalytical data of P(S-DVB) and ruthenium anchored catalysts**

| Compound | Degradation temperature (°C) | Wt. loss (%) |
|---|---|---|
| 5% P(S-DVB)$CH_2Cl$ | 478 | 33.0 |
| 8% P(S-DVB)$CH_2Cl$ | 469 | 31 0 |
| **Ru-A** | 381 | 28 4 |
| | 452 | 43 6 |
| **Ru-B** | 389 | 16 0 |
| **Ru-C** | 377 | 14 0 |
| **Ru-D** | 356 | 10 3 |
| | 432 | 24.8 |

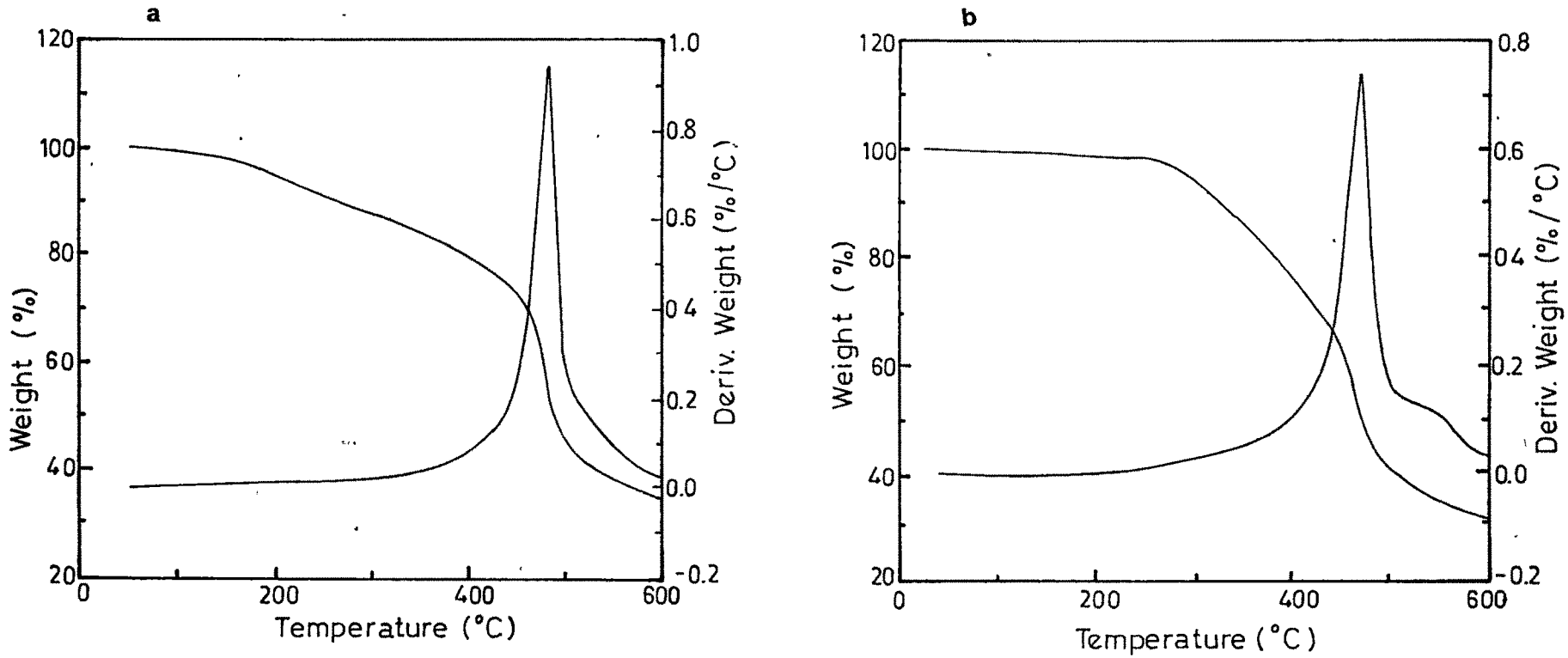


**Fig. 3.19 Thermograms of chloromethylated (a) 5% P(S-DVB) (b) 8% P(S-DVB)**

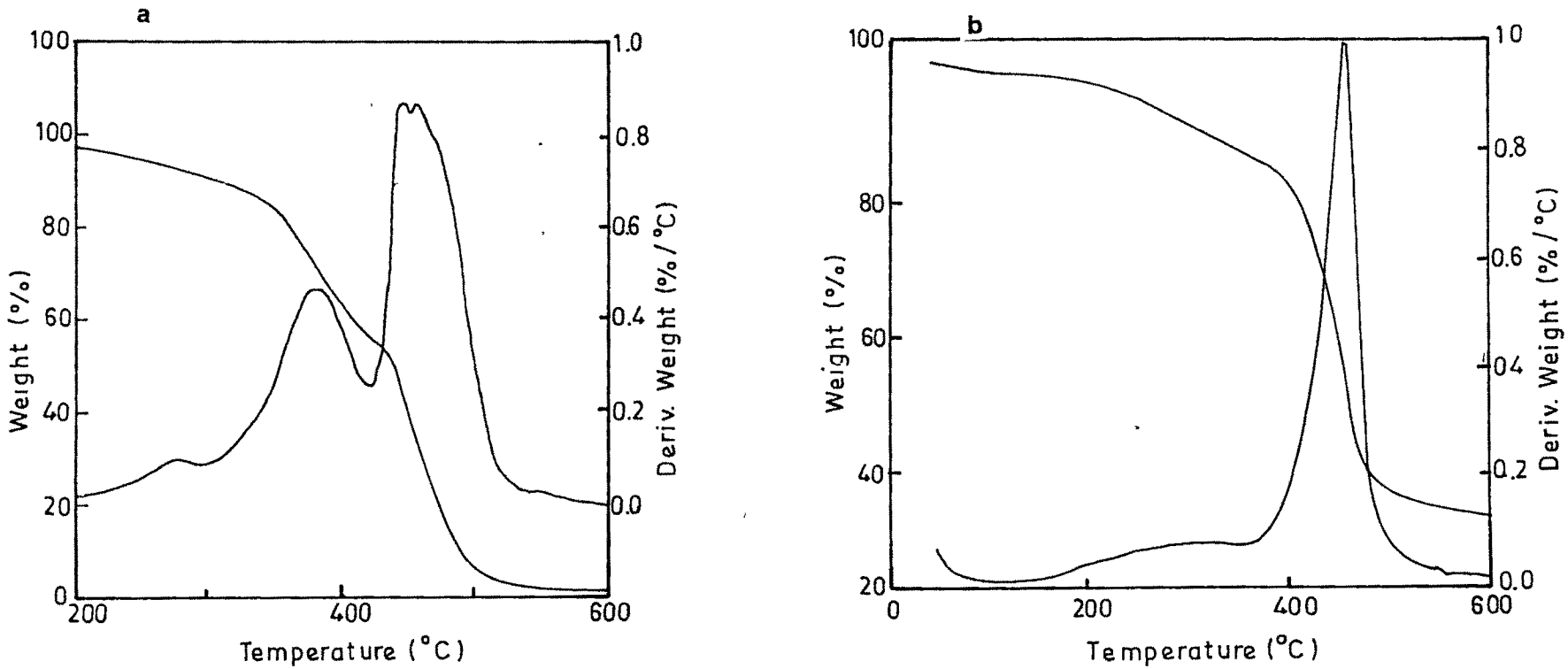


**Fig. 3.20(a) Thermograms of catalysts (a) Ru-A (b) Ru-B**

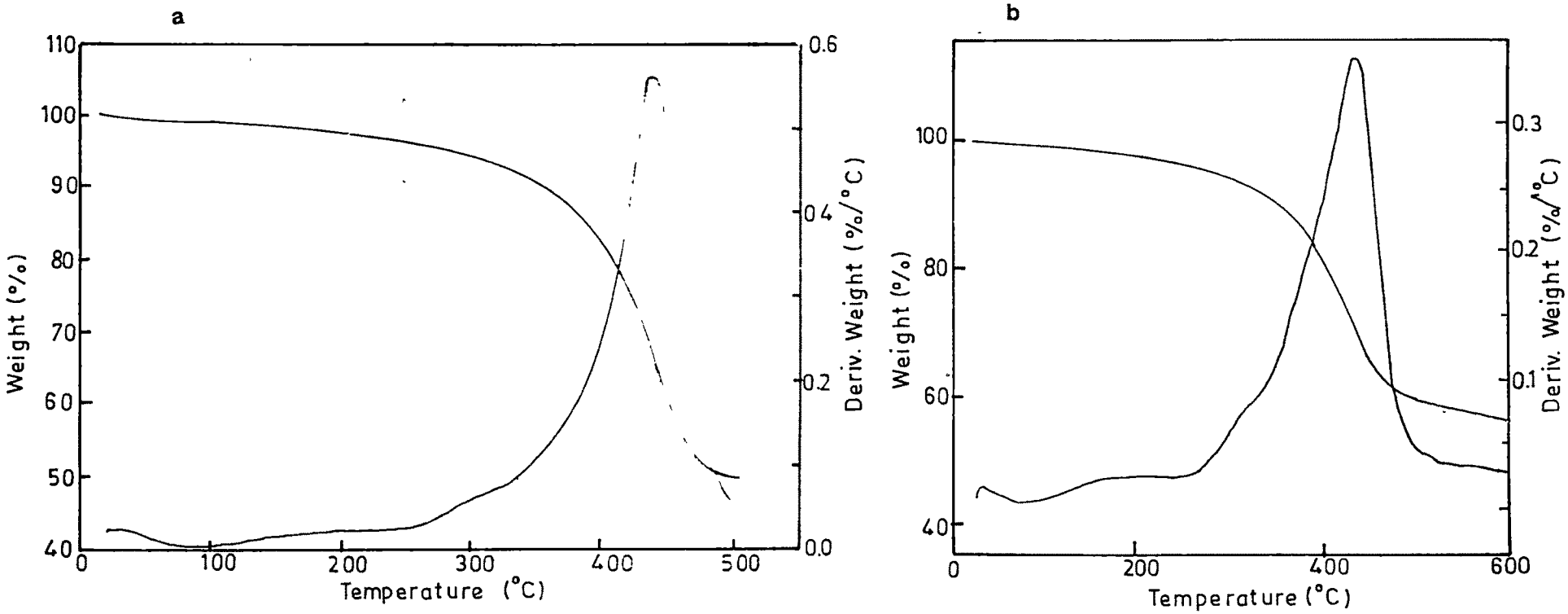


**Fig. 3.20(b) Thermograms of catalysts (a) Ru-C (b) Ru-D**

**Table 3.13**
**Thermoanalytical data of P(S-DVB) and manganese anchored catalysts**

| Compound | Degradation temperature (°C) | Wt. loss (%) |
|---|---|---|
| 5% P(S-DVB)$CH_2Cl$ | 478 | 33.0 |
| 8% P(S-DVB)$CH_2Cl$ | 469 | 31 0 |
| **Mn-A** | 420 | 31 1 |
| | 488 | 46 3 |
| **Mn-B** | 368 | 16 0 |
| | 449 | 40 7 |
| **Mn-C** | 384 | 14 9 |
| | 400 | 20 4 |
| **Mn-D** | 343 | 09 2 |

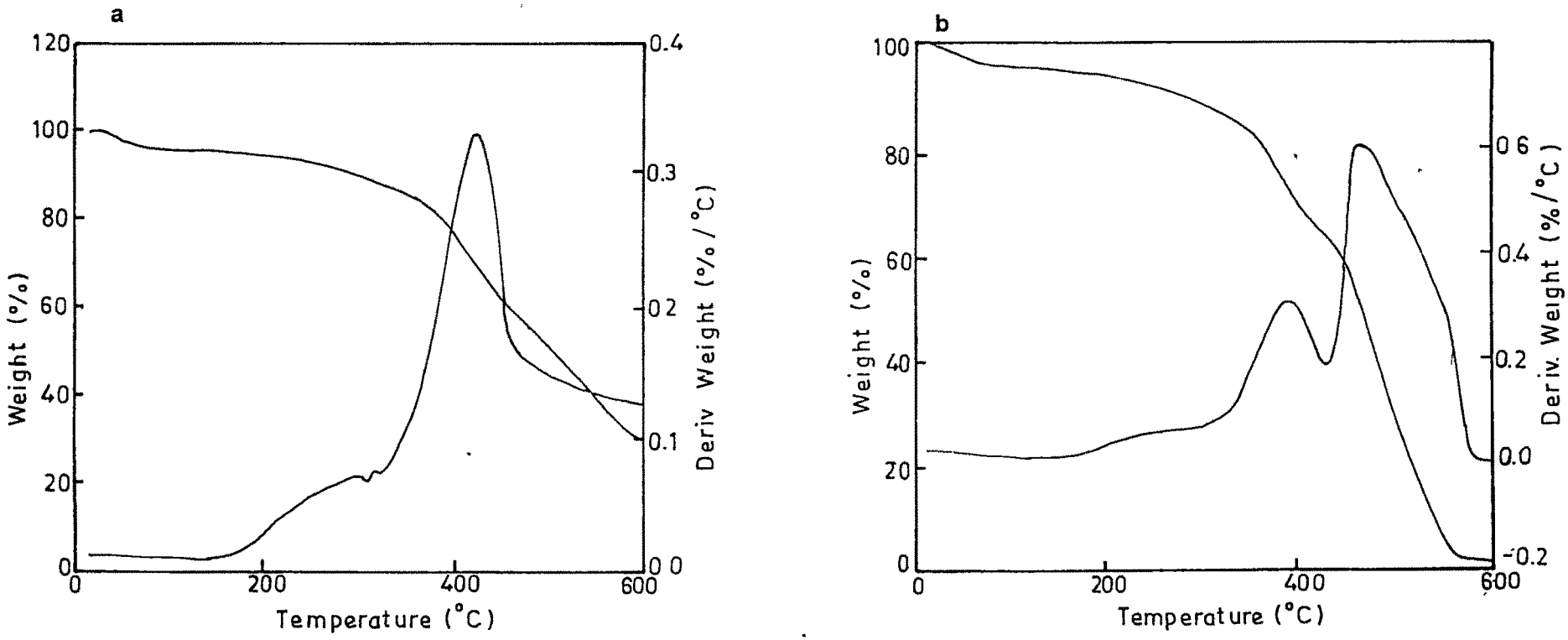


**Fig. 3.21(a) Thermograms of catalysts (a) Mn-A (b) Mn-B**

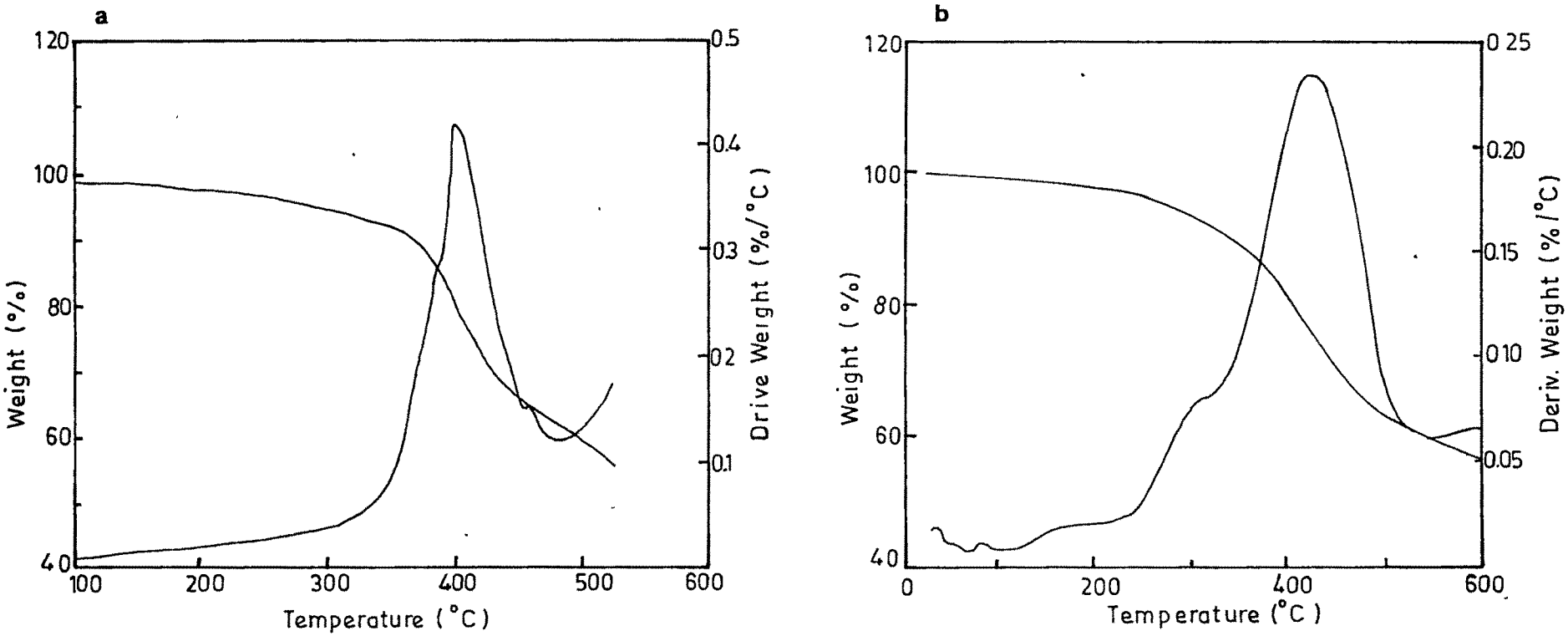


**Fig. 3.21(b) Thermograms of catalysts (a) Mn-C (b) Mn-D**

**Table 3.14**
**Thermoanalytical data of P(S-DVB) and palladium anchored catalysts**

| Compound | Degradation temperature (°C) | Wt. loss (%) |
|---|---|---|
| 5% P(S-DVB)$CH_2Cl$ | 478 | 33 0 |
| 8% P(S-DVB)$CH_2Cl$ | 469 | 31 0 |
| **Pd-A** | 380 | 16 8 |
| | 443 | 43 5 |
| **Pd-B** | 348 | 15 2 |
| **Pd-C** | 397 | 22 6 |
| **Pd-D** | 350 | 12 0 |
| | 435 | 25.0 |

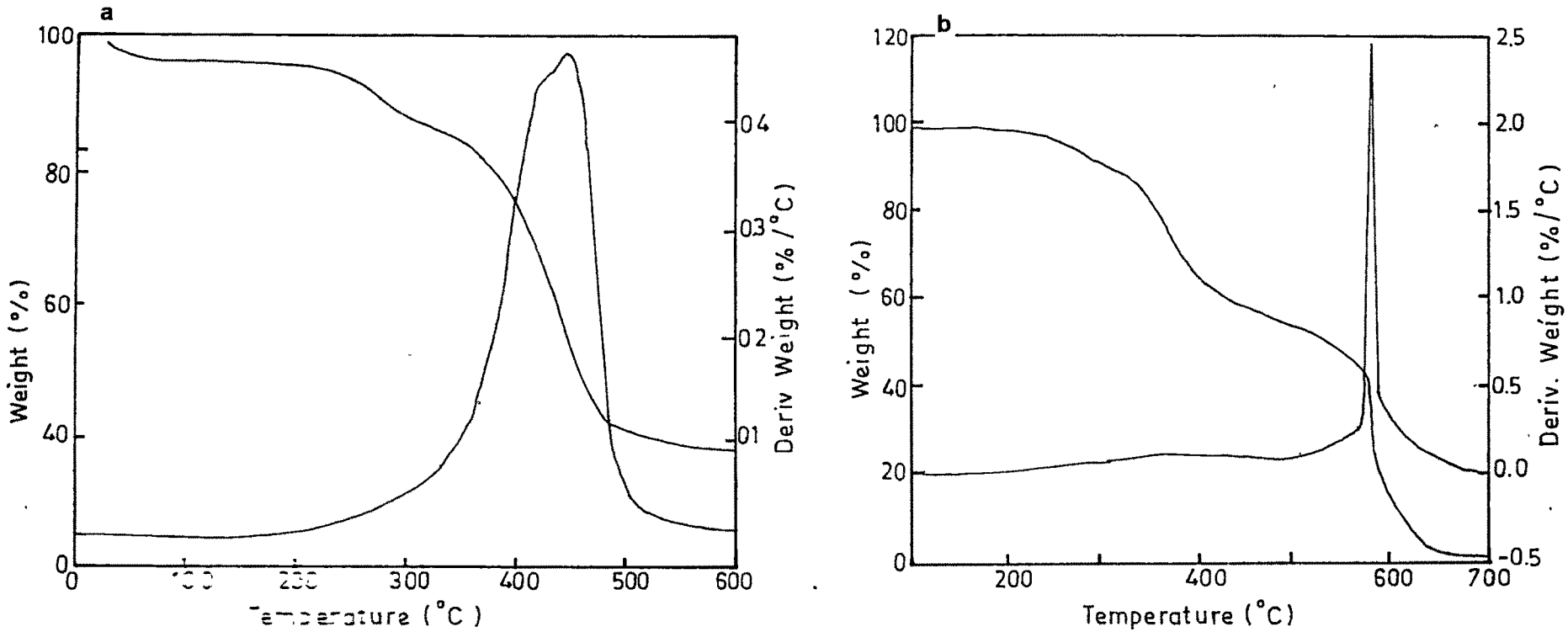


**Fig. 3.22(a) Thermograms of catalysts (a) Pd-A (b) Pd-B**

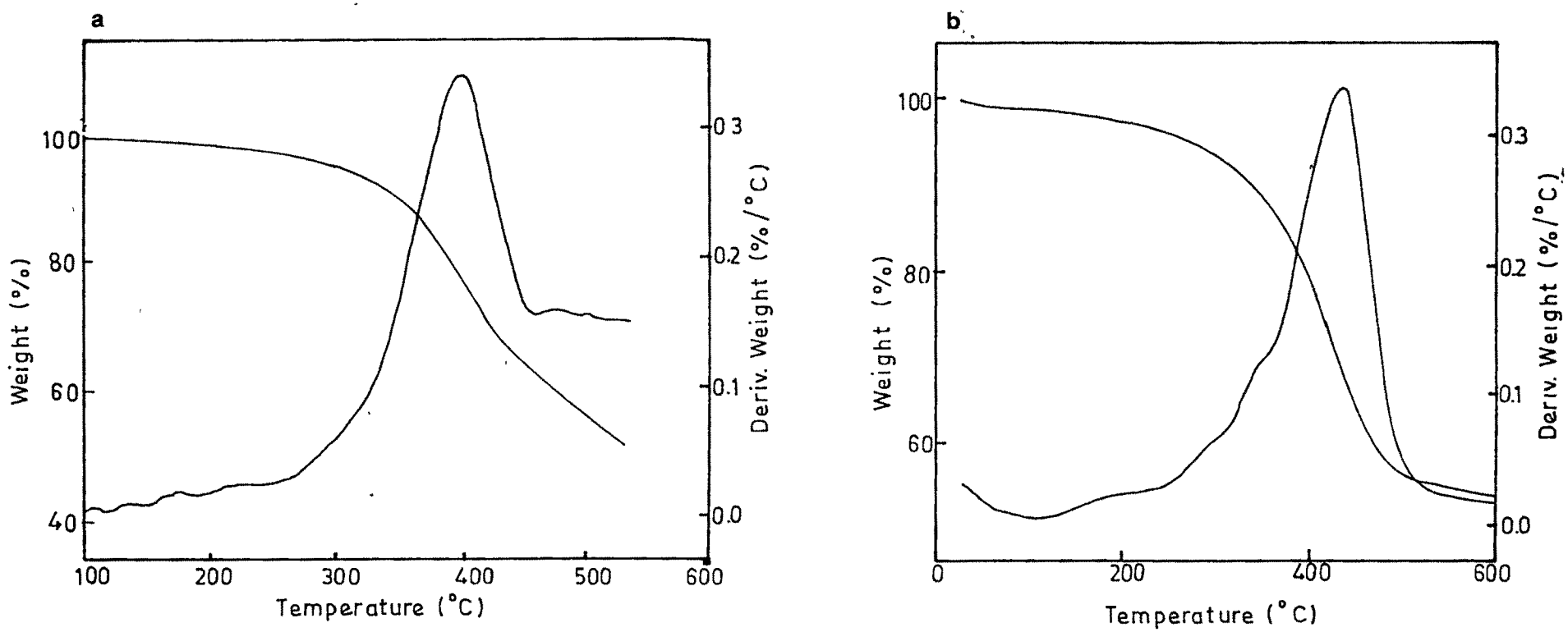


**Fig. 3.22(b) Thermograms of catalysts (a) Pd-C (b) Pd-D**

## 3.2 REFERENCES


[1] F. W Billmeyer, "*Textbook of Polymer Science*", Wiley Inter Science, NY , Third edition,(1979)

[2] R B Seymour, "*Introduction of Polymer Chemistry*" McGraw-Hill, NY, (1971)

[3] J. Haber, *Pure Appl Chem* 63,(1991),1227.

[4] D. T Gokak, B V Kamath and R N Ram, *J. Appl. Polymer Sci* , 35, (1988),1523

[5] D T. Gokak, B V Kamath and R N Ram, *Reactive Polymer*, 10,(1989), 37.

[6] J N Shah and R N Ram, *J Mol Catal* , 77,(1992),235

[7] R Antony, G L Tembe, M Ravindranathan and R. N. Ram, *J Mol Catal Chemical*, 171,(2001),159

[8] R Antony, G L Tembe, M Ravindranathan and R N Ram, *Polymer*, 19(18),(1998),4327

[9] S Schick, E Bartet and K. Dyrek, *Acta Polym* , 1,(1996),47

[10] G Kortum, "*Reflectance Spectroscopy, Principles, Methods and Application*", Springer-Verlag, Berlin, (1969)

[11] A B. P. Lever, "*Inorganic Electronic Spectroscopy*", Elsevier, NY, (1984)

[12] C V Gomes, M R Navarro and J R Masaquer, *Trans Met. Chem* , 9, (1984),52

[13] K Nakamoto," *Infrared and Raman Spectra of Inorganic and Coordination Compounds Part B Application in Coordination, Organometallic and Bioinorganic Chemistry* ", Wiley and Sons, Inc (1997),23.

[14] J R Thornback and J R Wilkinson, *J Chem. Soc* , Dalton Trans , (1978),110

[15] R A Nyquist and R O Kagel, "*The Handbook of Infrared and Raman Spectra of Inorganic Compounds and Organic Salts* " Vol 4, Academic Press, Inc , London, (1997)

[16] S Sasaki, Y Yanase, N Hagiwara, T Takeshila, H Naganuma, A O Hyoshi and K Ohkubo, *J Phys Chem. Soc* ,86,(1982),1038

[17] J V Sanders "*Catalysis, Science and Technology*" , J. R Anderson and M Bondart, (Eds ) Springer-Verlag, Berlin Heiddberg, 7,(1985),51

[18] P D Garm, "*Thermoanalytical Methods of Investigation*", Academic Press, NY, (1965)

[19] R C Mackenzie, "*Differential Thermal Analysis*", Academic Press, London, (1972)